TECHNOLOGICAL ATTRACTION POLES

FINAL REPORT

FLEXIBLE, ORGANIC SOLAR CELLS FOR POWER GENERATING TEXTILES
SOLTEX
PA-09

P. Heremans
IMEC

T. Meyvis
CENTEXBEL

Y. Geerts
Université Libre de Bruxelles

R. Lazzaroni
Université Mons-Hainaut

D. Vanderzande
Universiteit Hasselt

Rue de la Science 8
Wetenschapsstraat 8
B-1000 Brussels
Belgium
Tel: +32 (0)2 238 34 11 – Fax: +32 (0)2 230 59 12
http://www.belspo.be

Contact person:
Dimitri Harmegnies
Secretariat: +32 (0)2 238 37 61

TECHNOLOGICAL ATTRACTION POLES

FINAL REPORT

FLEXIBLE ORGANIC SOLAR CELLS FOR POWER-GENERATING TEXTILES

PA/09

Prof. P. Heremans – IMEC
Dr. Ir. T. Meyvis – CENTEXBEL
Prof. Y. Geerts – ULB
Prof. R. Lazzaroni – UMH
Prof. D. Vanderzande – UH

April 2006

Belgian Science Policy

Rue de la Science 8
Wetenschapsstraat 8
B-1000 Brussels
Belgium
Tel: +32 (0)2 238 34 11 – Fax: +32 (0)2 230 59 12
http://www.belspo.be

Contact person:
Dimitri Harmegnies
Secretariat: +32 (0)2 238 37 61

Table of contents

I. Context

Many new electronic technologies are being developed worldwide. They allow reducing production cost while increasing performance. The trend that is developing in our information society is that of omnipresent ("ubiquitous") and "wearable" electronic products. Wearable sensors, displays, computers, security, access control are some of the applications that are being researched. European industry is strongly aware of this, and actively involved in the development of goods and services for this market. Any of these electronic applications is necessarily powered electrically. There is, therefore, a strong demand for lightweight wearable power sources. Batteries are one form of power source. The use of non-rechargeable batteries in ubiquitously present electronics is not a sustainable option, the ecological consequences would be dramatic. Rechargeable batteries can be considered. But particularly attractive would be the integration of a wearable power source that generates electrical power from a universally present form of energy, for example light.

Solar cells are the means to convert light into electricity. Solar cells are made from semiconductors. Traditional semiconductors like silicon could to some extent be integrated in wearable products, but it would not be an affordable product that could truly be used for wearable electronics. In recent years, organic semiconductors have been developed that allow polymer (also called "plastic" or "organic") electronics products to be fabricated. These are lightweight, flexible, and low-cost. An additional benefit is that their production requires massively less energy that the production of conventional (mostly silicon) electronics, because by definition only low-temperature processes are used. Polymer solar cells are one of the electronic products that have successfully been demonstrated. They are an ideal candidate for a lightweight, extremely flat and flexible, autonomous electrical power source that can be integrated into clothing, baggage or accessories (backpacks, etc…) for powering wearable electronics – either directly or via rechargeable batteries.

In order to be successful for wearable electronics, the above-mentioned polymer solar cells must be integrated with the materials that are normally worn. Textile is the material of choice in this context.

Successful research and development in this area clearly requires a multidisciplinary team: plastic electronics is located at the borderline between chemistry and electronics manufacturing, and the integration with textile adds the latter industry to the mix.

Belgium has university groups, research institutes and industries that are actively involved in the plastic electronic revolution in the electronics arena. Belgium has a genuine interest in solar cell technology, with several industries producing such devices. Begium also has an important textile and clothing industry. With all these assets, Belgium has the potential to become an important player at the forefront of this new technological revolution, provided all these parties can be teamed together to work on a common goal. We have grouped in this consortium all chemistry Belgian university groups with an international reputation in the field of plastic electronics, together with the foremost electronic technology R&D center – who also has many years of experience

with development of polymer electronics – and the prime textile research center of the country. The user committee partners include the textile industry, the chemical industry, the solar-cell production industry, the electronics industry and the electrical power provider. This strong consortium allows us to reach the critical mass required for the enterprise, guarantees to keep the focus, ensures efficient transfer of knowledge from academics and R&D centers to industry, permits anchoring of know-how, expertise and brains within the country and within Europe, and will permit valorization of results in Belgium and Europe.

II. Project goals

From the several possible approaches to producing textile with integrated flexible solar cells, we have selected lamination as the preferred means of integration. Lamination is a procedure well-established and largely adopted by textile manufacturers. It allows a maximum freedom of the type of textile. It is compatible to the production of large areas. It provides genuine integration of the solar cell with the textile. It allows the textile manufacturer to be minimally involved in the production of the electronics part, in this case the solar cell.

The intended work consists of two main efforts. On the one hand, we will start from proven plastic solar cell technology and adapt this to achieve a solar-cell sheet that is suitable for lamination on textile. On the other hand, we will selectively replace certain parts of the solar cell in order to improve its performance in the demanded environment.

The proposed route of producing flexible solar cells on textile is by lamination. The substrate for the solar cell fabrication is a flexible plastic foil, like PET (poly-ethylene teraphtalate). The solar cell itself is of the bulk-heterojunction type, which has proven to have the highest efficiencies for plastic solar cells to date (about 3% efficiency under AM 1.5 when produced on glass). The layers of this type of cells are: an anode (likely PEDOT-PSS, a conductive transparent polymer), the active layer formed of a blend of an electron-conducting (PCBM) and a hole-conducting (e.g. MEH-PPV) material, and a cathode. This cathode will in first instance be aluminum. On top of this layer stack, we foresee a polymer barrier, e.g. based on polyurethane or parylene. The backside of the PET substrate can optionally also be coated with a similar barrier. This solar-cell-covered PET substrate then has to be laminated onto textile. The conditions of this lamination process have to be made compatible with the solar cell.

Ruggedness, UV resistance, lifetime and efficiency are critical issues in this application. In parallel to early work on lamination of state-of-the-art cells described above onto textile, we foresee work on the improvement of these critical parameters. For ruggedness and UV resistance, we will test several coating materials, both on top of the cathode and at the bottom of the PET substrate. Lifetime of the cell will in part be limited by UV resistance, but also by the diffusion of water (vapour) and oxygen – both to be blocked by suitable coatings – and also by the lamination process and, most importantly, by the polymers in the active layer. To improve on the latter, work is foreseen on new materials, in particular hole transport materials. The efficiency of plastic solar cells today is mostly limited by the poor match between the absorption spectrum of the cells (dictated by the material choice) and the emission spectrum of the sun. The new materials mentioned above will therefore also be designed to provide an absorption spectrum that better matches the solar spectrum.

III. Results

A. Partner IMEC

1. Processing

Screen-printing is studied as deposition technique for conjugated material based layers. Photovoltaics based on the principle of bulk donor-acceptor heterojunction are tested using a blend of poly(2-methoxy-5-(2'-ethyl-hexyloxy)-1,4-phenylene vinylene) (MEH-PPV) mixed with the C60-derivative (6,6)-phenyl C61-butyric acid methyl ester (PCBM). First, different solution concentrations of the donor MEH-PPV material and of the blend are subjected to rheology measurements. Addition of the acceptor (PCBM) to a donor material based solution induces a decrease of the solution viscosity. However, the overall flow behaviour of the blend remains similar to that of the MEH-PPV based solution. Secondly, it is shown that specific printer settings have to be used to obtain active layers that are suitable for opto-electronic applications. Finally, devices with an overall energy conversion efficiency of 1.25% under standardized simulated solar illumination (AM1.5G; 100mW/cm2) have been obtained showing that screen-printing can be a suitable technique for the deposition of the active layer of polymer solar cells.

Solar cells with conjugated materials as active layer have the potential to compete with standard Si-based photovoltaics when production costs are taken into account. The possible use of low-cost substrates as well as the necessity of only a very thin organic active layer leads to a substantial materials cost reduction. Moreover, chemical modifications of the materials such that they become soluble in common solvents make it possible to exploit solution based processes to deposit the active layer, reducing the production costs even further. A common technique to process such conjugated materials is spin coating. In this way, a thin, homogeneous film is easily applied onto large substrates. However, no direct patterning of the deposited layer can be obtained by this technique. Using printing techniques to process organic materials offers the opportunity to obtain patterned films directly onto the substrate. Inkjet printing has in this way already shown its suitability to prepare multi-color displays. The high resolution and the small features that come in reach makes inkjet printing even suitable for fabrication of full plastic transistors. Nevertheless, processing organic solar cells probably does not require this high precision and may need a process with higher throughput. Therefore, screen-printing as a linear casting technique can be interesting as a novel deposition technique to process organic photovoltaics. Moreover, the patterning of the film in one step will even facilitate the production of solar cell modules and the integration of the photovoltaic device into several application tools like smart cards, mobile phones …

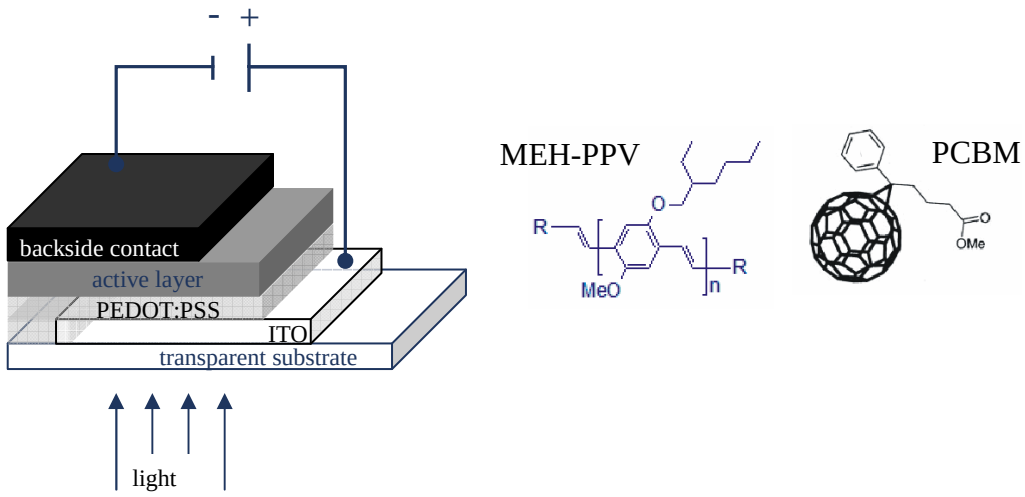

Figure 1: Schematic representation of bulk donor/acceptor heterojunction solar cell with the chemical structure of the materials in the active layer

One of the most promising concepts is that of the bulk donor-acceptor (D/A) heterojunction solar cell, based on the principle of ultrafast (subpicosecond) photo-induced charge transfer from a conjugated polymer to a fullerene (C60) molecule. Blending the donor and acceptor material an interpenetrating bi-continuous network is formed such that generated charges can be transported towards their respective contacts. IndiumTinOxyde (ITO) covered with a thin layer of poly(ethylenedioxythiopene)/poly(styrene-sulfonate) (PEDOT/PSS) is commonly used as transparent electrode whereas evaporated metals like Ca or LiF/Al form the backside contact (see Fig. 1). Processing is almost fully independent of the substrate material and can be done on glass as well as on e.g. poly(ethylene therephtalate) (PET) foils. The latter offers the opportunity to produce fully flexible solar cells due to the mechanical flexibility of the organic active layer.
To study the feasibility of screen-printing as a deposition technique for the active layer, poly(2-methoxy-5-(2'-ethyl-hexyloxy)-1,4-phenylene vinylene) (MEH-PPV) is used as donor material, whereas the acceptor is the C60-derivative (6,6)-phenyl C61-butyric acid methyl ester (PCBM). Chemical structures of these compounds are given in Fig. 1. Both materials can be dissolved in common organic solvents such that processing of the blend from solution is possible. Rheology measurements on polymer based solutions as well as on blends are performed to see what the effect is of the addition of PCBM to the donor based solution. However, optimising and studying the influence of printing parameters is also important. This is first done with a single component solution containing only the donor material. In a later stage, screen-printing of D/A blends is done, to achieve photovoltaic devices. It is shown that screen-printing can be a suitable deposition technique for the active layer of polymer solar cells. Moreover, the direct patterning of the deposited layer will facilitate the production of photovoltaic modules.

a) Rheology measurements

Rheological measurements were carried out on a Carri-Med Rheometer (CSL2 500) with a cone/plate measuring system such that the shear rate γ is constant over the full surface of the geometer. This equipment allows studying the viscosity η as function of the shear rate γ and the temperature T. We have examined solutions with different concentrations of the MEH-PPV polymer as well as a blend of the donor and acceptor material in a ¼ weight ratio. The solvent was chosen to be in all cases chlorobenzene (CB) as it was proven to be beneficial for the performance of the actual solar cell.
Fig. 2 depicts the result of a rheological measurement for different solutions at a constant shear rate of 100/s but whereby the temperature was gradually varied from 10°C to 55°C. For all these solutions it can be observed that the viscosity increases when the temperature is lowered. However, no strong increase is seen, showing that no gelation is appearing in this temperature range for any of these solutions. Taking the three uppermost curves into account, the variation of the viscosity for different polymer concentrations is shown. The 1% (w/v) concentrated MEH-PPV solution has a viscosity ranging from 7x10-2 Pa.s at 10°C to 4x10-2 Pa.s at 55°C. These values triple when the concentration is doubled and even increase almost 12 times for 3% concentrated solutions. It was not possible to study the behaviour of higher concentrated MEH-PPV solutions due to limited solubility of the polymer in chlorobenzene.
The lower curve in Fig. 2 shows the behaviour of a 1% polymer solution to which PCBM is added in a ¼ ratio by weight. Also in this case, the viscosity increases when the temperature is raised without any appearance of gelation in the applied temperature range. Remarkably, the values vary from 3x10-2 Pa.s at 10°C to 1.6x10-2 Pa.s at 55°C being lower than what was obtained for the pure 1% MEH-PPV solution. So, the viscosity decreases despite the addition of solid material.

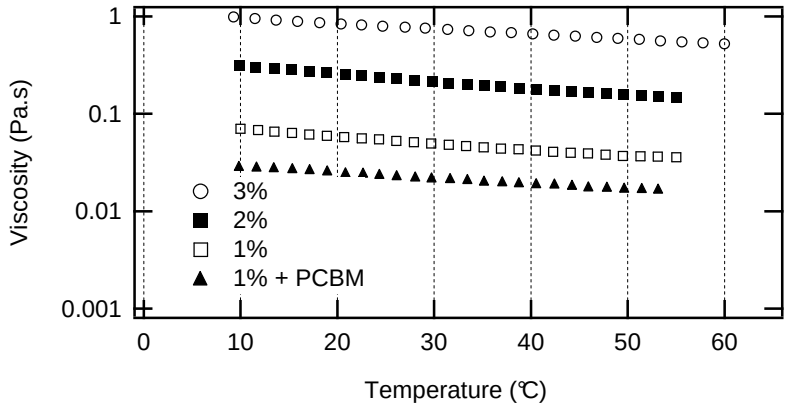

Figure 2: Viscosity measured as function of temperature for different polymer solution concentrations and for a donor/acceptor blend solution

Fig. 3a shows the result of a measurement on the 1% polymer solution whereby the shear rate was varied. This was done for different temperatures ranging from 10°C to 55°C. It can again be observed that the viscosity increases when the temperature is lowered.

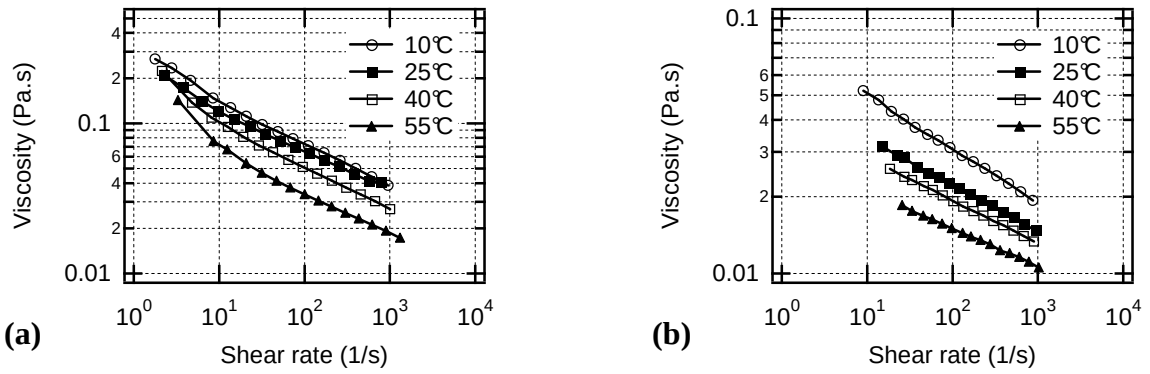

Figure 3: Viscosity as function of applied shear rate for different temperatures for (a) 1% MEH-PPV solution and (b) 1% MEH-PPV solution with additional PCBM in a ¼ weight ratio

Furthermore, there is a clear dependence of the viscosity upon the shear rate in such a way that η decreases for higher γ values. This type of flow behaviour is often called shear-thinning or pseudo-plastic and can be caused by a strong interaction between the polymer chains in the solution.
A similar measurement is performed on the 1% concentrated solution after the addition of PCBM in a ¼ weight ratio. The result is given in Fig. 3b, showing also in this case the same temperature dependence as measured before. If we compare the values of the blend with those obtained for the pure polymer solution, we see that the viscosity is lower for the blend, under similar measurement conditions. This confirms the observation of the previous measurement. Due to the fact that PCBM is a rather small molecule with respect to the long polymer chains of MEH-PPV it appears to have a weakening effect on the pure solution. In this way the interaction between the polymer chains is reduced leading to a decrease of viscosity. However, it can be observed from Fig. 3 that for the blend the viscosity still depends on the applied shear rate. So, the addition of PCBM decreases the viscosity of the solution but the overall pseudoplastic flow behaviour remains.

b) Devices with screen-printed active layer

Fig. 4a depicts the basics of the screen-printing process. The screen, consisting of woven wires of e.g. nylon, polyester or stainless steel, is attached onto a frame. The desired printing pattern is defined onto the screen by applying specific emulsion coatings, thereby filling the openings in the screen in the areas where no ink is supposed to be deposited. The screen is then placed above the substrate at a certain offset (or snap off) distance. By moving the squeegee, the ink is spread over the screen. Applying sufficient pressure onto the squeegee, it deflects the screen downward to make contact with the substrate. The ink is then forced through the open areas of the screen not filled by the emulsion coating onto the substrate. As the squeegee passes a given point, screen fabric tension snaps the screen back, leaving the ink behind.
The experiments described further on were all carried out using a manually operated SP002-R screen printer (ESSEMTEC) with a polyurethane squeegee (shore hardness 85),

set at an angle of 45°. Polyester screens where commercially bought (KOENEN Gmbh) with an open printing pattern of 4.5cm by 4.5cm. The printing itself is done in ambient atmosphere. Due to the photovoltaic application we are studying, the substrates were always glass sheets (5cm by 5cm) covered with ITO on which a 30nm thin layer of PEDOT/PSS is spin coated.

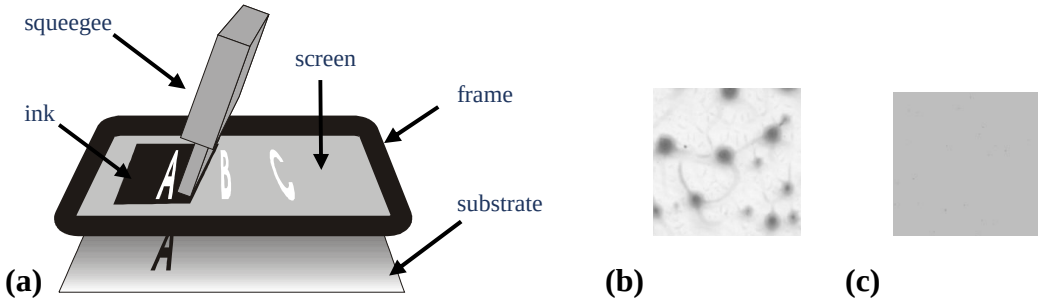

Figure 4: (a) Basic scheme of the screen-printing process, and digital scans (0.8cm by 0.8cm) of screen-printed layers of MEH-PPV with (b) low speed and (c) high speed of the squeegee movement

Concerning the machine set-up, we focused on variables like the printing speed, the snap off distance and the squeegee pressure. Screens with different mesh sizes, i.e. the number of wires per cm, were also studied. The influence of these different printer settings on the film formation and thickness was examined for solutions containing only the donor material MEH-PPV.

It turned out that the speed of movement of the squeegee had the most serious influence on the film morphology. Photographs of such MEH-PPV layers printed at low and at high speed are given in Fig. 4. The film after printing with low speed of the squeegee movement is non-homogeneous with very uneven spreading of the material over the substrate. Areas with almost no material present are contrasting with places of thick droplet-like zones. On the other hand, when a sufficiently high printing speed is applied a much more homogeneous film is formed (see Fig. 4c). Even coverage of the substrate and good spreading of the material is observed in this case. Therefore, all subsequent results are obtained by printing at high speed of the squeegee movement. The effect of the snap off distance, the squeegee pressure and the mesh size on the final print result was already reported elsewhere.

In accordance with these experiments, we have fabricated photovoltaic devices with a screen-printed active layer. We used a donor/acceptor blend based on a 1% MEH-PPV solution with additional PCBM in a ¼ weight ratio. The ITO film on the glass substrates was patterned beforehand by UV-photolithography. Prior to the printing of the polymer solution, a thin PEDOT/PSS layer was spin coated on these patterned substrates. To finalize the device structure, a metallic backside contact of LiF/Al was evaporated in high vacuum (~10-8 Torr) on top of the active layer through a shadow mask. In this way, solar cells were fabricated with active areas ranging from 0.09cm2 to 0.47cm2.

Typical current-voltage (I-V) characteristics of such device are presented in Fig. 5, as well in dark as under standardized simulated solar illumination (AM1.5G, 100mW/cm2). For the dark IV-curve clear diode behaviour is observed with a rectification ratio of over 103 at 2V. Under illumination a short circuit current density Jsc of 3.4 mA/cm2, an open circuit voltage Voc equal to 845 mV and a fill factor FF of 44% is obtained. This results

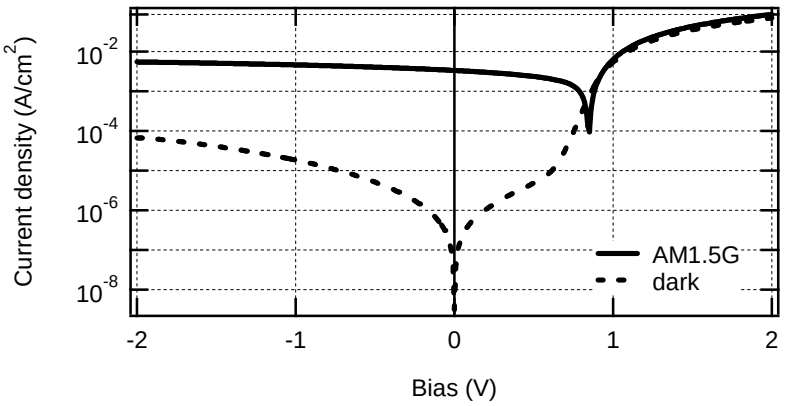

Figure 5: Current-Voltage characteristic of a bulk donor/acceptor heterojunction solar cell with screen-printed active layer in dark and under standardized simulated solar illumination (AM1.5G; 100mW/cm2)

in an overall energy conversion efficiency of 1.25%. This is almost comparable to standard spin coated PPV/C60 based solar cells.

(a) (b)

Figure 1: (a) digital scan of an MEH-PPV film screen printed at a speed of 150mm/s; (b) color histogram of the same film

However, optimising and studying the influence of printing parameters is still very important. It was already shown that higher printing speeds resulted in more homogeneous films. Further investigation was done on this effect. Therefore, different solutions have been printed varying the printing speed from 150mm/s up to 550mm/s. Digital scans of the resulting films were made and these were analysed by making color histograms. Such a histogram expresses for each color intensity (X-axis) the number of pixels having this intensity (Y-axis). An example is given in Figure 1.

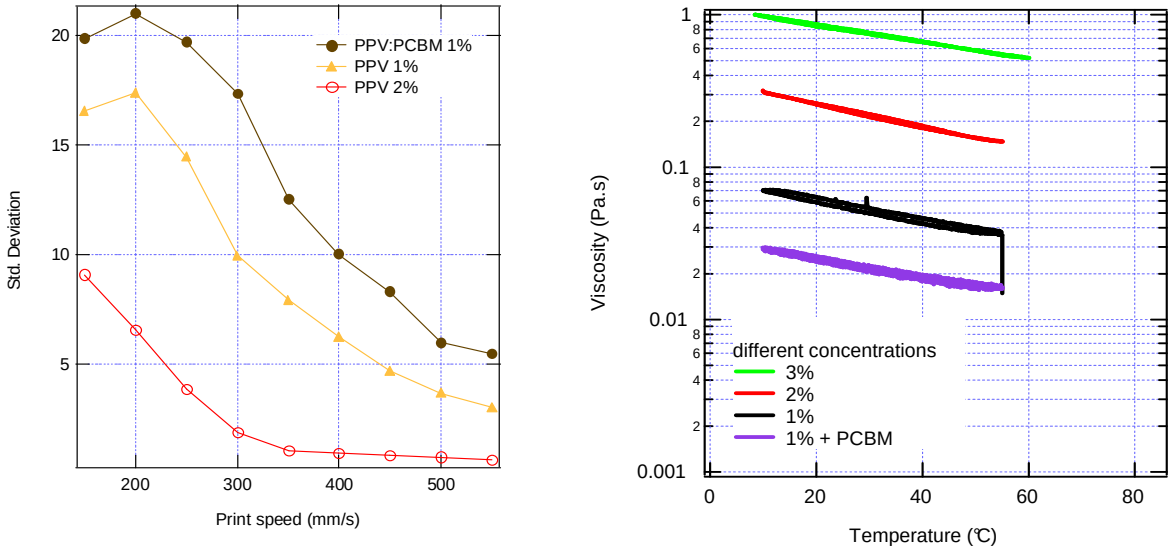

(a) (b)

Figure 2: (a) Calculated standard deviations from color histograms of screen printed films of MEH-PPV and MEH-PPV:PCBM solutions as function of the print speed; (b) Viscosity as function of the temperature for MEH-PPV and MEH-PPV:PCBM solutions

For the distribution as given in such a histogram, the mean value or the median expresses the general color of the print. The calculated standard deviation of each histogram is a good measure for the overall homogeneity of the picture. In this way, printed films of 2% MEH-PPV, 1% MEH-PPV and 1% MEH-PPV:PCBM (1:4) solutions from chlorobenzene have been analysed. The result is shown in Figure 2(a) representing the calculated standard deviations as function of printing speed for the different solutions. The improvement of the film quality with increased printing speed is now quantitatively expressed by the clear decrease of the standard deviation. Figure 2(b) depicts the result of a rheological measurement for different solutions at a constant shear rate of 100/s. The temperature was gradually varied from 10°C to 55°C. It shows that the viscosity of these solutions decreases with decreasing polymer concentration or upon addition of PCBM. The standard deviations as shown in Figure 2(a) decrease similarly with increasing viscosity. This might indicate that the printing speed becomes less important for more viscous solutions.

A possible phenomenological explanation might therefore be as follows. If the viscosity of the solution expresses its cohesion then the observed behavior shows that the film formation might be strongly influenced by the interplay between these cohesion forces and the adhesion of the solution to the screen. The adhesion effect results in inhomogeneous deposition of the solution. By applying a higher printing speed, the screen snaps off faster such that adhesion of the solution onto the screen can be prevented. Therefore, a higher printing speed overcomes this effect.

Since the screen printing technique is introduced to obtain organic solar cell modules we have progressed also in this way. Therefore, first attempts have been made to process also on flexible foil. Patterning of the transparent and backside electrode was similar to the glass substrate. An active layer of MEH-PPV:PCBM (1:4) was deposited by screen printing. Measurement under simulated solar illumination (AM1.5G, 100mW/cm2) yielded a maximum overall energy conversion efficiency of 0.65%. The reduction in efficiency on flexible substrates with respect to glass is strongly caused by an increased series resistance, partly explained by a higher resistive ITO-layer. We have also observed imperfections at the backside contact if processed on flexible foil. This might be caused by thermal stress on the substrate during evaporation of the metal contact. So, more appropriate conditions have to be determined for this process step.

(a)

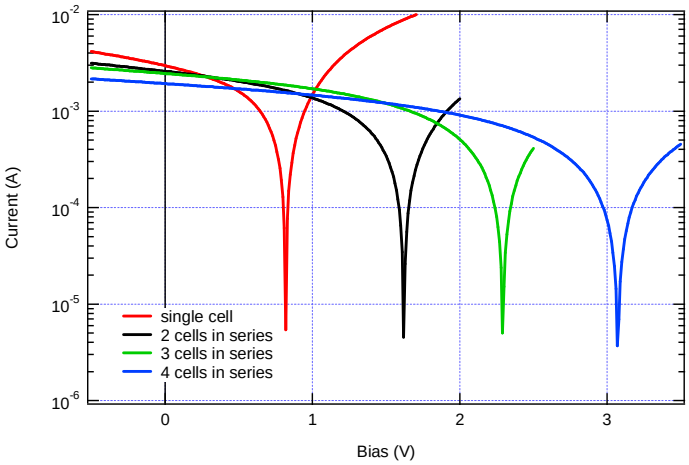

(b)

Figure 3: (a) Picture of a photovoltaic module on a flexible substrate with a screen printed active layer of MEH-PPV:PCBM; (b) Current-Voltage characteristic of the flexible photovoltaic module under AM1.5G simulated solar illumination (100mW/cm2)

Nevertheless, photovoltaic modules with a printed active layer of MEH-PPV:PCBM were processed on flexible substrates. Figure 3(a) shows a picture of such a device with four cells with an active area of ~2cm2 each. By connecting the cells in series, the output voltage is increased to achieve a total open circuit voltage over 3V under simulated solar illumination (see Figure 3(b)).

This shows that processing on flexible substrates is also possible and that a flexible solar cell module on a single substrate can be produced, facilitating the integration of such devices into specific applications. Based on such a flexible organic module a demonstrator was fabricated to illustrate and promote the project. A suitcase from Samsonite with a textile part was used to integrate a small LCD display powered by solar cell modules.

2. Exploring new materials

For the characterization of new materials two main contributions can be described. At first, the liquid crystalline material H2Pc-O-(14,10)4 has been thoroughly investigated, as well electrically as morphologically. Secondly the P3HT polymer was thoroughly investigated as a new donor material in the bulk heterojunction solar cell with a C60-fullerene derivative as acceptor.

a) Discotic liquid crystal

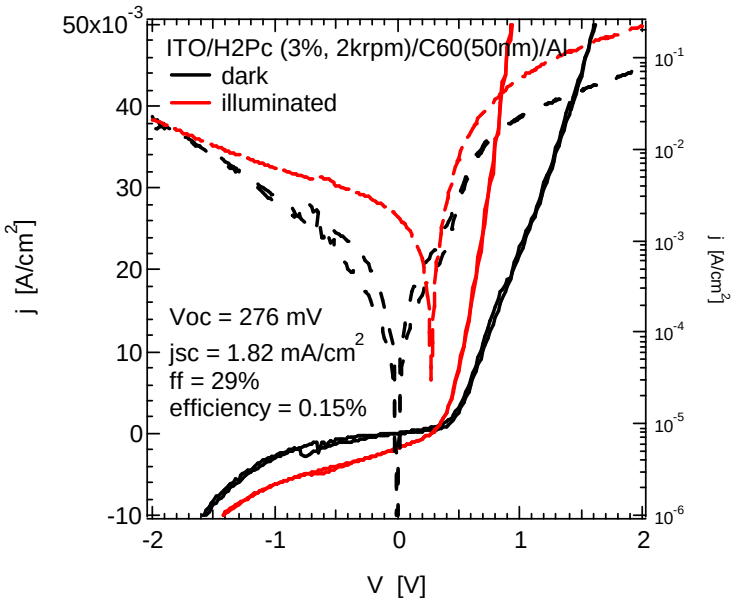

Figure 9: Current-voltage characteristics of a ITO/H2Pc/C60/Al thin film diode in darkness and under illumination with 100mW/cm2.

At IMEC, we fabricated and characterized thin films of the discotic liquid crystal H2Pc(14,10)4, synthesized by Yves Geerts group at ULB, using a temporary PVP layer on top of the discotic for aiding the homeotropic alignment. The discotic was spin-coated from a toluene solution (e.g. 30mg/ml at 2000rpm) on an ITO substrate. Subsequently, PVP was spin-coated from a methanol solution in order to provide a second surface for aiding the alignment of the discotic liquid crystal. After annealing the sample at about 180°C in the isotropic phase of the discotic, followed by a slow cool-down to the liquid-crystalline phase with homeotropic alignment, the PVP layer was washed off with methanol. In order to investigate the photovoltaic action, a 50nm thin C60 layer and Al electrodes were evaporated on top. The current-voltage characteristics are shown in Figure 9. The photocurrent of this ITO/ H2Pc(14,10)4/C60/Al diode is higher than for a C60 single layer diode, demonstrating the contribution of the discotic liquid crystal to the generation of photocarriers. In comparison, non-aligned H2Pc(14,10)4/C60 diodes show almost two orders lower photocurrents. However, we have indications that the aligned

discotic is damaged (i.e. becomes partly disordered) by the thermal evaporation of the subsequent layer. The evaporation of Al directly on top of the discotic yielded current-voltage characteristics which were similar for films with aligned and non-aligned H2Pc(14,10)4. Even C60, evaporated at only 300°C, seemed to degrade the H2Pc(14,10)4/C60 interface, despite the substrate cooling with liquid nitrogen.

In order to characterize the charge carrier mobility of the discotic in a field-effect transistor configuration, we collaborated with the Max-Planck-Institute für Polymerforschung, Mainz, in order to align the H2Pc(14,10)4 columns parallel to the substrate surface. For this purpose, a top glass plate was introduced into the total sample configuration. The SiO2 substrate and the top glass plate are treated with OTS in order to promote the homogeneous alignment of the discotic. First tests are shown in the micrograph shown in Figure 40: an H2Pc(14,10)4 film was sandwiched between two OTS-treated glass plates, and then locally annealed along a certain axis by the zone recrystallization method. The result shows that the intended alignment could be achieved. However, the processing of films sandwiched between Si/SiO2 and top glass for the transistor configuration turned out to be complicated by the different thermal conductivities. More optimisations are necessary in order to fabricate working field effect transistors with homeogeneously aligned H2Pc discotics.

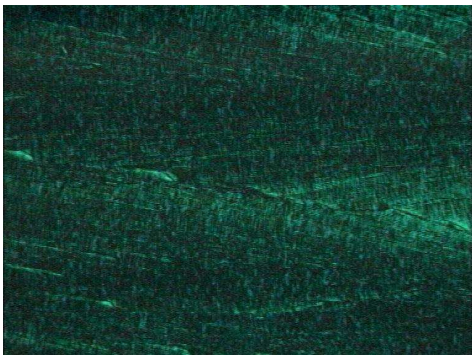

Figure 40: Cross-polarisation micrograph of a zone-crystallised H2Pc thick film between two OTS-treated glass plates.

b) Low bandgap polymer P3HT

Regioregular poly(3-hexylthiophene-2,5-diyl) (P3HT) is a semiconducting polymer which has been studied already extensively in organic transistor research and shows, due to its crystalline properties, interestingly high mobilities. The fact that organic solar cells are limited in thickness due to low mobilities of the constituents + the smaller bandgap of P3HT compared to the well known solar cell polymer PPV and the abundant availability of P3HT (commercialized by Rieke Metals inc.) made P3HT an interesting candidate as donor material for organic solar cells.

Earlier in this work it has been shown that solar cells can be made with this material from chlorobenzene solutions of P3HT/PCBM blends and that the power conversion efficiency can be improved dramatically upon thermal annealing with an optimum annealing temperature of 100 C. It was found that in part this has to do with a red-shift in absorption.
In a further investigation at IMEC the active layer was studied in more detail to get more insight in what the reasons are for the improvement of the solar cell characteristics upon annealing.

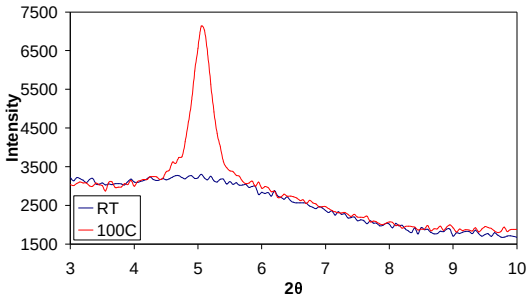

Figure 5: XRD-pattern of 1/2-blend P3HT/PCBM before and after annealing

XRD and Electron diffraction patterns measured with TEM showed a clear effect of the blend composition and annealing treatment on the film crystallinity. As an example the XRD diffractograms of an as-produced 1:2 blend and after annealing at 100 C for 5 minutes are given in Figure 511. The as-produced film is amorphous while the annealed film shows a distinct diffraction peak originating from P3HT crystals.
Recently we have been able to detect an effect of annealing on images of the layer morphology taken with TEM. In case of the 1:1 blend the as-produced film shows a homogeneous phase, while after annealing at 100 C for 5 minutes grainlike P3HT crystals with 10 x 30 nm dimensions appear (Figure 16). This is an indication of phase separation between P3HT and PCBM upon annealing.

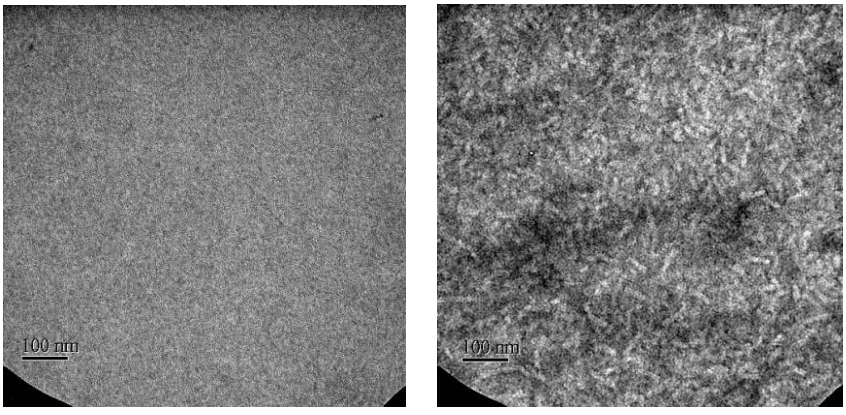

Figure 16: TEM images of a 1:1 blend film a) as-produced and b) after annealing at 100 C, 5 minutes.

At that point it was clear that crystallinity of the film could be improved upon annealing and that this reflected in the change of absorption spectrum before and after annealing. The question then was whether this also had implications on the charge carrier mobilities in the active layer. For that electron and hole mobilities were extracted from field effect transistor (FET) measurements. Results obtained from transistors with aluminum source and drain contacts showed indeed a gradual increase in hole mobility with increasing annealing temperature (Figure). An activation temperature of between 50 and 80 C was seen. This activation temperature is consistent with earlier absorption spectrum measurements in which was found that the absorption spectrum of 1:2 blend films started changing when heated above 70 C.

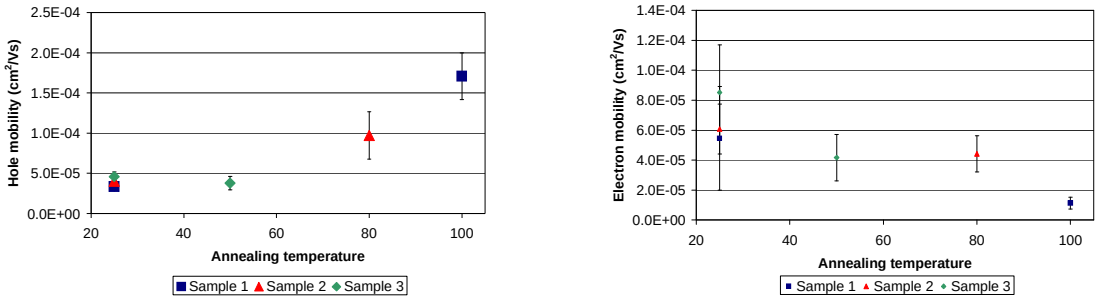

Figure 13: a) Hole mobilities and b) electron mobilities of 1/2-blend P3HT/PCBM determined in FET-structures

After a full optimization of the chlorobenzene based devices, a power conversion efficiency of 2.7% was the best result obtained. In order to further improve the efficiency, the use of solvents other than chlorobenzene was investigated. This approach was chosen since in earlier research in the field of bulk heterojunction organic solar cells it was found that the solvent used during the device production plays a major role in the eventual device performance. From this study an additional element was found. The desired P3HT crystallinity is influenced by the drying time of the active layer during production. It was found that by playing with the boiling point of the solvent the film drying time could be influenced. In this way it was possible to obtain a power conversion efficiency of 4.3% with as-produced devices. Annealing of those devices has become obsolete.

3. Summary

On the level of processing, the feasibility of screen printing as a deposition technique for the active layer of organic polymer based bulk heterojunction solar cells has been evaluated. It was shown that as well single devices as monolithic modules could be fabricated with this technique. A blended layer of MEH-PPV and PCBM was used as standard for this investigation. Single cells with an efficiency >1.25% could be produced. Modules in which a series connection of several single cells was achieved on a flexible

substrate showed an output voltage of >3V, sufficient to drive small applications like a calculator...
Based on such a flexible organic module a demonstrator was fabricated to illustrate and promote the project. A suitcase from Samsonite with a textile part was used to integrate a small LCD display powered by solar cell modules.

The very stringent properties requested for the encapsulation of organic solar cells made it difficult to obtain a fully optimized processing on flexible foil at this stage. Nevertheless, state-of-the-art flexible substrates with very specific barrier layers were identified as potential encapsulation materials for the organic solar cells.

For the characterization of new materials two main contributions can be described. At first, the liquid crystalline material H2Pc-O-(14,10)4 has been thoroughly investigated, as well electrically as morphologically. Very restrictive processing conditions made this investigation rather difficult. Nevertheless, mobility as well as solar cell measurements were achieved. Mobility values in the order of 10^{-4} to 10^{-3} cm^2/Vs could be identified by SCLC and TOF measurements. For photovoltaic devices, it was shown that the best performance could be obtained only with a bilayer configuration with C_{60} as acceptor material instead of a fully mixed active layer. An efficiency of 0.15% was measured for this device.

Secondly the P3HT polymer was thoroughly investigated as a new donor material in the bulk heterojunction solar cell with a C_{60}-fullerene derivative as acceptor. It has been shown that solar cells can be made with this material from chlorobenzene solutions and that the power conversion efficiency can be improved dramatically upon thermal annealing. After a full optimization of this chlorobenzene based devices, a power conversion efficiency of 2.7% was obtained. In a further investigation the active layer was studied in more detail combining absorption measurements with morphological techniques like TEM and XRD and electrical mobility measurements. The use of solvents other than chlorobenzene showed that it was possible to obtain a power conversion efficiency of 4.3% with as-produced devices. Annealing of those devices has become obsolete.

B. Partner CENTEXBEL

1. Protection layers

During the project the search was ongoing for suitable protection layers. Coatings do not come anywhere near the oxygen and water diffusion limits wanted therefore only films where studied. The currently used PET barrier film treated with the Barix™ from VitexSystems can be stated as state of the art. During the Barix™ process alternating layers of inorganic material deposited by plasma and UV-curable polymers are deposited on the substrate. This process can not be applied directly to the solar cells because of the needed intense UV exposure for curing. Contacts with Alcan revealed the existence of a film in development stage based on their Ceramis brand. After investigation diffusion limit for oxygen was no lower than 0,1 cm^3/m^2dbarand therefore still far from the set limits. At the Fraunhofer Institut für Silikatforschung (Würzburg, G) current research focuses on a combination of Silica based levelling film (sol-gel) combined with a sputtered metal layer and finished with a hybrib sol-gel layer containing fluor. Using this technology oxygen diffusion van be obtained lower than 0,01 cm^3/m^2dbar but so far no commercial products where available. Therefore it was decided to concentrate on the encapsulation of the solar cells by applying another layer of barrier PET film. Further evolution will be discussed in the Task 3 Encapsulation..

2. Design (contacts)

Table 1 Overview of possible soldering compositions

SOLDER COMPOSITION	MELTING POINT	COMMENTS
48 Sn/52 In	118°C eutectic	Low melting point, expensive, low strength
42 Sn/58 Bi	138°C eutectic	Established, availability concern of Bi
91 Sn/9 Zn	199°C eutectic	High drossing, corrosion potential
93.5 Sn/3 Sb/2 Bi/1.5 Cu	218°C eutectic	High strength, excellent thermal fatigue
95.5 Sn/3.5 Ag/1 Zn	218°-221°C	High strength, good thermal fatigue
99.3 Sn/0.7 Cu	227°C	High strength and high melting point
95 Sn/5 Sb	232-240°C	Good shear strength and thermal fatigue
65 Sn/25 Ag/10 Sb	233°C	Motorola patent, high strength
97 Sn/2 Cu/0.8 Sb/0.2 Ag	226-228°C	High melting point
96.5 Sn/3.5 Ag	221°C eutectic	High strength and high melting point

Contacts had to be designed that can be ideally produced in a roll to roll process. On the textile, current transport can be done by actual wires but also printed circuits. Wires can be connected by soldering although the temperature sensistivity of the plastic solar cells clearly limits the possibilities. From
Table 1 the limited availability and quality of low temperature (< 200°C) solderings is evident .

Sewing is a traditional textile technology but not very suited because of the high risk to disrupt or delaminate the solar cell. Electrically conductive glues can be prepared using carbon black or silver particles. Main restriction of glues is the needed solvent evaporation which will certainly be a problem when using impermeable textiles (eg coated textiles). A third option is to create a contact strip on the side of the solar cell that can be inserted into a flexible PCB connector connected to conductive wires in the textile. This option limits the design and fabrication possibilities of the solar cells and problems can be expected in moist conditions.
The best solution seems to be to perforate the PET to a well defined depth (mechanically or with a laser) and to introduce a conductive paste in the created hole. As conductive paste, silver (10-4 Ohm/cm), copper or conducting polymer pastes like PEDOT/carbon black (7.10-3 Ohm/cm) can be used. In order to limit the amounts of contacts to be interconnected on large surfaces the current can be transferred from the contacts to a conductive circuit that collects the current. This circuit can be attached to the solar cell assembly or can be situated on the textile.

A promising alternative is the use of modified push-trough buttons. As illustrated in Figure 7 they can make a connection between conductive layers on different substrates. A circuit could be printed on the textile conducting the current directly to the point where it is needed and all individual solar modules could be connected to this circuit with push-trough buttons.

In this setup the textile needs to be specially prepared (conductive circuit) in order to be able to host solar cells. In another setup the original idea of perforating the base PET foil and introducing a conductive paste as contact was used to design solar cells with integrated glueing and circuitry solutions (see Task 3).

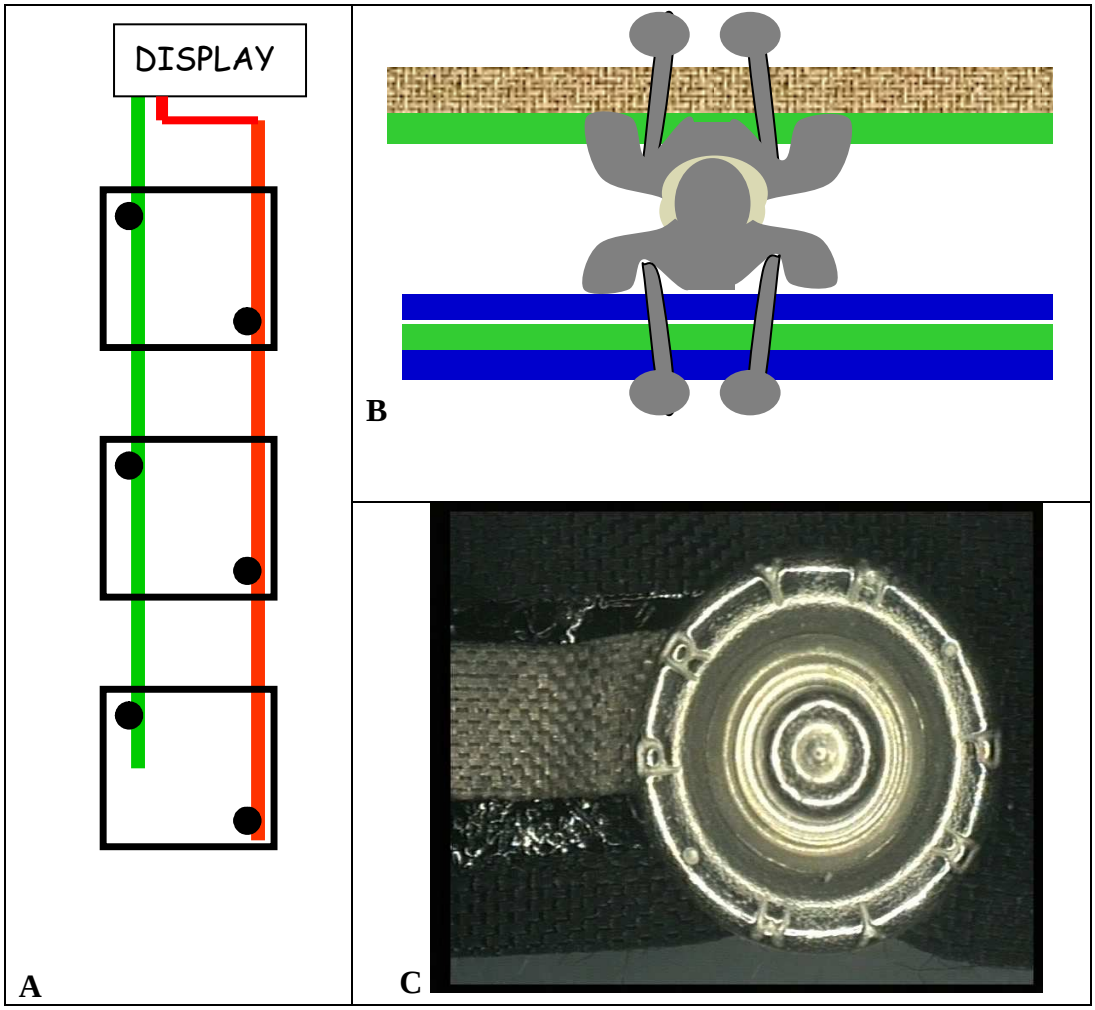

Figure 7 Schematic illustration of solar cell modules connected to a circuit on a textiles by push-through buttons (A), schematic cross section of a push-through button ((B) green represents contacts or conductive layers) picture of such a system applied to a textile with a conductive layer (C).

3. Fabrication

a) Patterning

It was the ultimate goal to produce the solar cells on a roll to roll process. This means that depending on the previewed application parts will be cut from the roll and individually laminated to the textiles or for large surfaces a roll to roll lamination will be

used. The patterning should be done in such a way that the produced roll of solar-cells can be used for both small and large scale applications. As illustrated schematically in the picture the solar-cell roll should be build from base units that will be interlinked by a conductive circuit to limit the needed contact points. The conductive circuit can be printed on the back of the solar cell or on an adhesive tape (which revealed to be a suitable solution for laminating) that is laminated to the back of the solar cell or on the textile (using push-through buttons as contacts). This would result in lines (in the direction of production) of interlinked base units. A base unit has two contacts and generates enough power for the most basic applications e.g. a calculator. The base unit may consist of several solar-cells but it is essential that it only has two contacts. Based on current research results the surface of such a base unit would be about 25 cm². By producing in this way every thinkable size (limited by the size of the base units) can be cut from the roll. When large areas are used only a limited amount of contact points (situated at the side of the solar-cell assembly) are needed to transfer the generated current to a device.

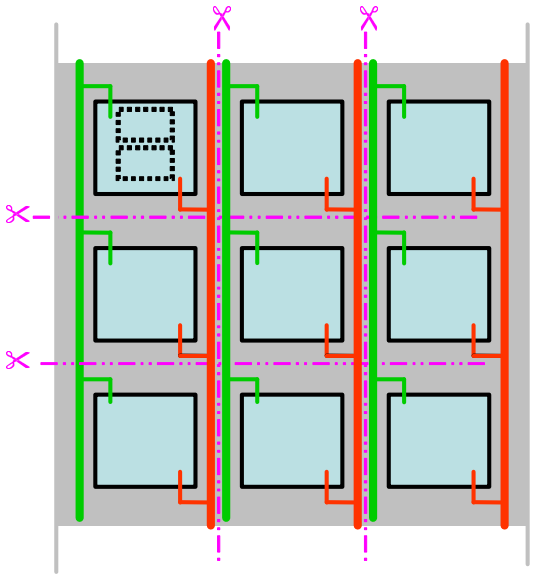

Figure 2 Schematic illustration of the layout of solar cell modules interconnected by a circuit to collect the current and dividable in various sized solar cell assemblies.

Pursuing the idea of push-through buttons for contacting the need of a printed circuit on the back of the solar cells or the adhesive no longer exists. The patterning can remain but the collection of the current can be done by a circuit printed on the textile that is directly linked to the application. In this case each base unit is connected to the circuit with two push through buttons Figure 7 (A). This technology would also eliminate the need for perforation of the solar cells and consecutive application of a conductive paste.

To apply conductive circuits to textiles screen printing, digital printing, sputtering and electrochemical deposition techniques can be used. None of them however are currently state of the art. At the ITCF in Denkendorf (G) electroconducting inks suitable for digital

printing based on graphite particles and a UV-curable polymer where prepared and tested. With a carbon black content of 10% a non-metallic conductivity level could be obtained. Centexbel has performed experiments with sputtering and screen printing.

For the sputtering a mask with various patterns was made. In the first experiments the mask was fixed on a plastic film and an Al-layer (40' Al, ~1µm) and a Cu- layer (30' Cu, ~1µm) where sputtered. Due to deformation of the mask and the permeability of the substrate the resolution was not good.

In a second phase Al and Cu layers where deposited as a band on different textile materials. Even when using tapes for masking the resolution of the deposition was variable due to the surface irregularity of the textiles. Single layers (1 µm) showed no measurable conductivity nor did double layers. Only when a layer was applied to both sides of the textile a resistance of 100 kOhm could be measured.

Screen printing experiments with an electroconductive ink where performed on cotton and polyester samples using a screen with various elements and curing for 10 minutes at 110°C. As can be seen from Figure 8 the resolution is very good and even very fine elements can be printed.

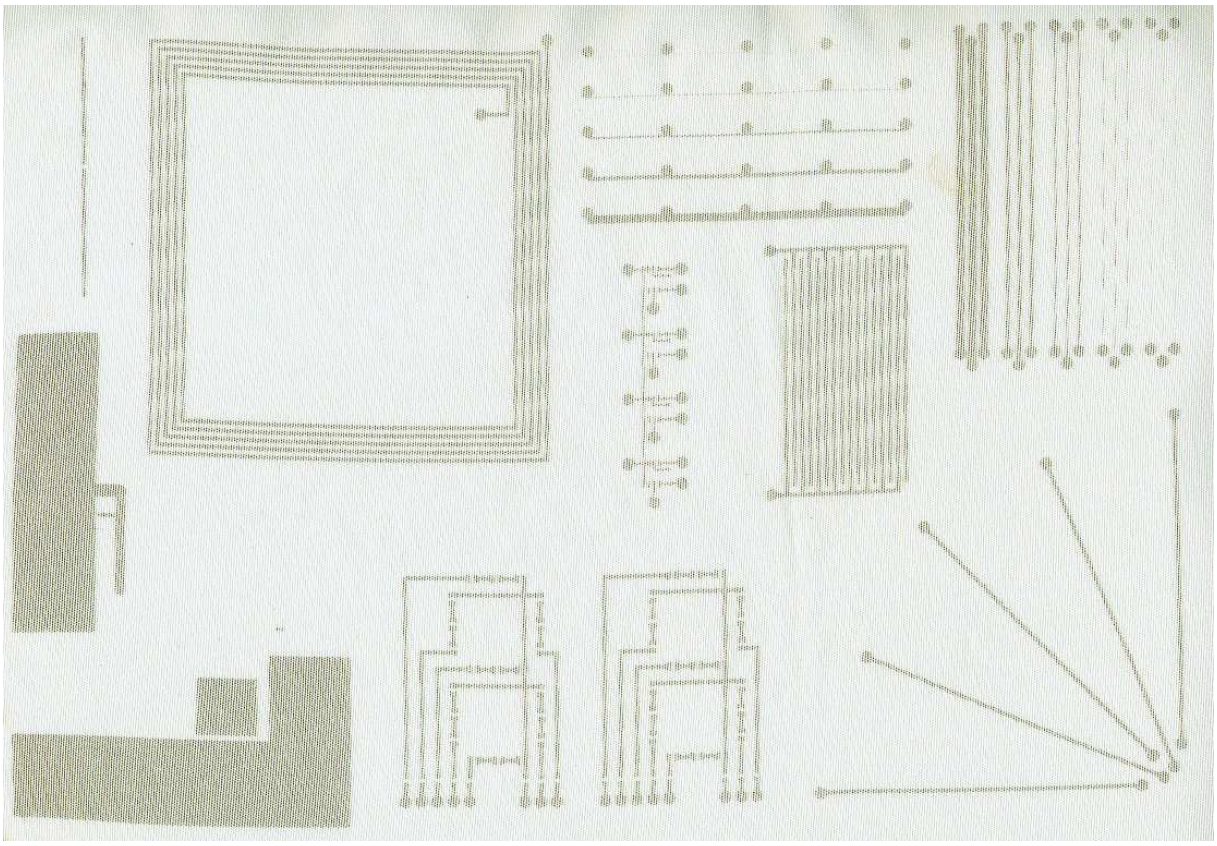

Figure 8 Conductive elements screen printed on polyester

One layer however was not enough to show conductivity. Because the sensitivity of textiles towards deformation during thermal treatments further optimalisation is needed in order to be able to apply thicker layers in one run.

b) Encapsulation

For encapsulation of the solar cells it was decided to use the same special PET film used as substrate for the solar cells since it is the only available film that guaranties minimum water and oxygen permeation. In order to seal the solar cells both PET sheets have to glued together. The easiest way to perform this sealing is to use a glue over the entire surface of the PET films. Cyanoacrylates are very efficient but aggressive glues that attack the surface. Since the glue is put on top of the solar cell build-up this is likely to cause damage. In fact all glues that demand solvent evaporation are not suited because of the total impermeability of the PET foil. Therefore thermoplastic polyurethanes where evaluated. These where applied as a solvent based coating on a PET barrier film. After drying the coated film was pressure laminated to a non coated PET barrier film (representing the film with deposited solar cell) at 150°C. After optimalisation of the coating composition an adhesive strength of 12 N/cm could be obtained which is acceptable. When laminating two barrier films water and oxygen diffusion can still occur at the glue layer through the thermoplastic polyurethane. In order to limit the water

diffusion the use of molecular sieves as additives for the coating was tested. Mixing of the sieves in the thermoplastic polyurethane formulation worked well and uniform dispersions up to 10% could be prepared. Coating on PET barrier film was similar with or without molecular sieves. Coatings with molecular sieves showed a more irregular surface after drying. Lamination of a coated PET barrier film with a non-coated using hot-air welding resulted in laminates with decreasing adhesion as the level of molecular sieves in the coatings was increased. After optimalisation of the dispersion the reduction in adhesion could be limited to an acceptable level for 5% molecular sieves.

Hot melts also classify as possible laminating glue but the lack of clear thermal restrictions for the treatment of the solar cells limits the possibilities.

c) Lamination

For the lamination PET foil was chosen as a model substrate. It was laminated to various types (polyester, polyamide, PVC) of textiles provided by the industrial partners. Three types of lamination were tested: wet with polyurethane and epoxy resins (melamine and isocyanurate crosslinkers); film lamination with polyurethane films and powder lamination with EVA, polyethylene, polyurethane and polyester powders. Best results were obtained with the powders and more specific with the polyester type Optimal powder add-ons where situated between 120-150 g/m² depending on the substrate and corona pre-treatment of the substrates could not substantially lower this amount nor increase the adhesion significantly. During the project it became clear that thermal treatments can play an important role in the preconditioning of the active layers of the solar cells limiting the thermal conditions usable during lamination.

It was decided to change the lamination strategy in order to avoid intensive heat treatments needed for curing. In stead of laminating the solar cells directly to a textile, the solar cells will be laminated roll to roll on a double sided adhesive tape. The ultimate goal is to produce a roll of self-adhesive plastic solar cells that can be cut to size and sticked to the desired substrate (a textile or any other surface). Pressure sensitive tapes based on modified acrylics gave the most promising results for laminating PET barrier film to textiles. With the best tape laminates where made between textiles (pvc and pp) and an ITO coated PET film and the durability of the adhesion was tested in a QUV testing apparatus simulating outdoor conditions (UVA 340 nm, 60°C + condensation cycle (50°C)). From Figure 9 it can be deducted that the weathering stability of the laminates is rather good.

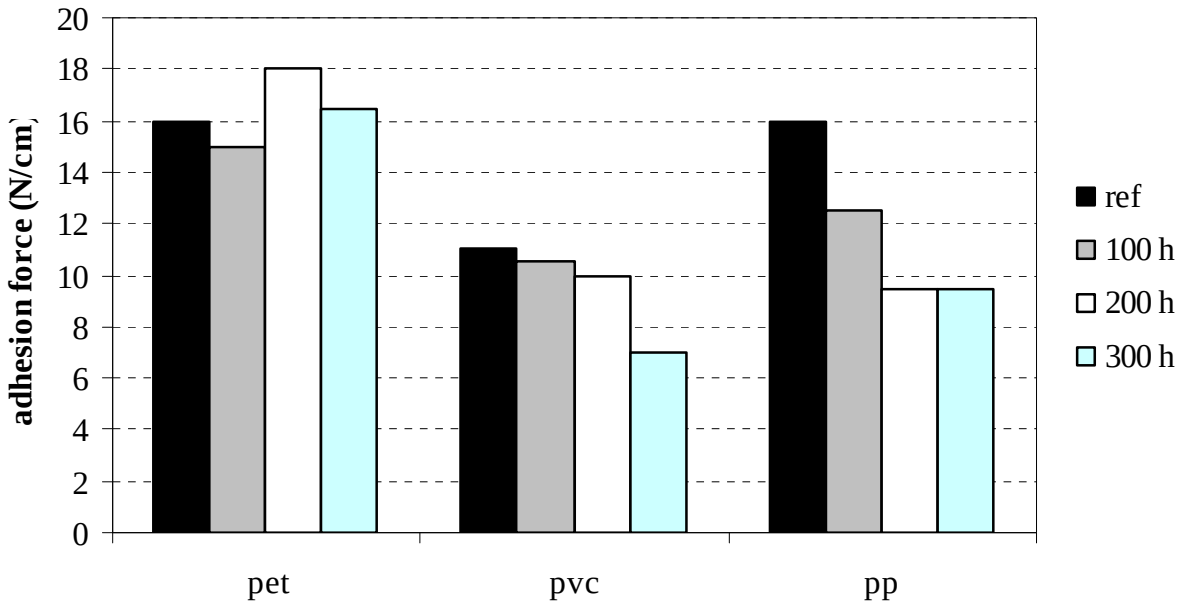

Figure 9 Weathering stability of various laminates

The laminate with pp shows a typical UV degradation behaviour with an initial strong drop in adhesion strength followed by a stabilisation. The slowly decreasing adhesion with pvc is probably caused by migrating weakening agents. The pet-pet laminate is perfectly stable showing that the degradation of the strength is mainly caused by the weakening of the textile and not the degradation of the PSA. PSA's proved to be preferment enough for lamination of plastic solar cells to various (coated/non-coated and different materials) textile substrates. A viable alternative could be hot-melt technology but the thermal restrictions of the solar cells should be well defined first.

C. Partner UNIVERSITE LIBRE DE BRUXELLES

1. Materials

The liquid crystal selected by ULB as the most promising candidate for the design of solar cells was a tetra alkyloxy-substituted phthalocyanine H2Pc-O-(14,10)4 with the chemical structure presented in the figure 1. It is a p-type semiconducting materials, i.e. which carry positive charges. Since it was demonstrated in the literature that photo-induced electron transfer was very efficient between phthalocyanine and fullerene 1, a soluble fullerene derivative, [6,6]-phenyl C61-butyric acid methyl ester (PCBM) (figure 1b) was selected as electron acceptor

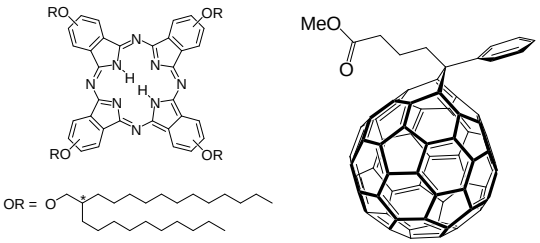

*Figure 1: Chemical structure (a) of mesogenic four-fold substituted phthalocyanine (**H_2Pc-O-(14,10)$_4$**) that exist as a mixture of four isomers : D_{2h}:C_s:C_{2v}:C_{4h} with a statistical distribution 12.5:50:25:12.5. Alkoxy side chains have been used as racemates; (b) of phenyl-C_{61}-butyric acid methyl ester (**PCBM**).*

2. Synthesis

PCBM is a commercial product available at Nano-C, 33 Southwest Park, Westwood, MA 02090, USA.

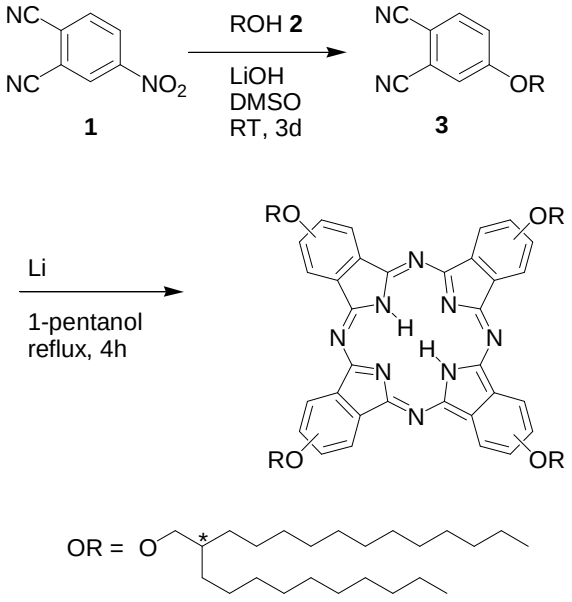

Scheme 1. Synthetic pathway to tetraalkoxyphthalocyanine

The synthesis of Pcs H2Pc-O-(14,10)4 has been performed in two steps, as depicted in Scheme 1. The nitro group of the commercially available 4-nitrophthalonitrile 1 undergoes a nucleophilic substitution by the alcohol 3 in dimethylsulfoxide in presence of lithium hydroxide. This step has been carried out using a previously reported method, yielding 50-54 % of 3 after purification. 2 When 1 are stored at room temperature (RT), the slightly yellow oils gradually turn to a slight green color. The cyclotetramerisation of 4-alkoxyphthalonitrile 3 in presence of metallic lithium affords H2Pc-O-(14,10)4 obtained as dark green pasty materials, in yields ranging from 43 to 50 % after purification by column chromatography. Organic solvents of various polarity such as tetrahydrofuran, methylene chloride, toluene, and hexane solubilizes well H2Pc-O-(14,10)4. The UV-visible, 1H NMR, and MS spectral characteristics of H2Pc-O-(14,10)4 are in agreement with their chemical structures. The metal-free character of the H2Pc-O-(14,10)4 and its full chemical structure are confirmed by several techniques :

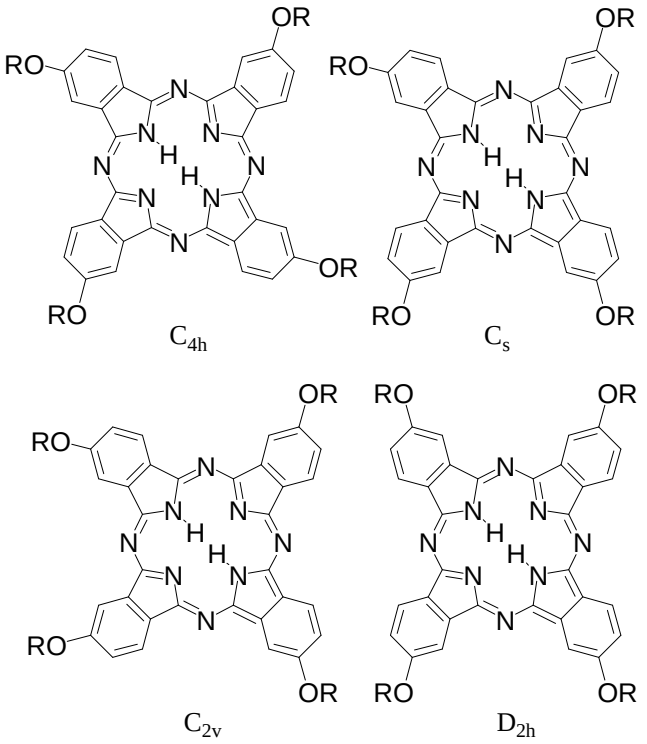

Scheme 2. ***H_2Pc-O-(14,10)$_4$*** *exists as a mixture of four isomers : D_{2h}:C_s:C_{2v}:C_{4h} with a statistical distribution 12.5:50:25:12.5, Alkoxy side chains have been used as racemates.*

- Field desorption mass spectrometry : 962 (M^+/2), 1924 (M^+), 2564 ($4M^+$/3), 2886 ($3M^+$/2), 3207 ($5M^+$/3), 3366 ($7M^+$/4).
- Nuclear magnetic reasonance of protons : 1H NMR (C6D6) : δ (ppm) –3.1 (br, 2 H), 0.91 (m, 24 H), 1.3-2.0 (m, 120 H), 2.1 (br, 2 H), 2.2 (br, 2 H), 4.10 (br, 4H), 4.32 (br, 4 H), 7.55-7.76 (m, 4 H), 8.56-8.73 (m, 4 H), 9.01-9.20 (m, 4 H). The three sets of signals observed in the aromatic region of the 1H NMR spectra

reveal the presence of a mixture of isomers (Scheme 2). Aggregation in solution has complicated in the characterization see below.

- UV-visible spectroscopy (toluene): □max (□) = 705 nm (149000 ± 15000 L.mol-1.cm-1), □ (□) = 671 nm (146000 ± 15000 L.mol-1.cm-1), □ (□) = 344 nm (129000 ± 15000 L.mol-1.cm-1).

Aggregation in solution has been probed by 1H NMR. Figure 2a-b shows the effect of aggregation on the 1H NMR spectra as a function of solvent and temperature

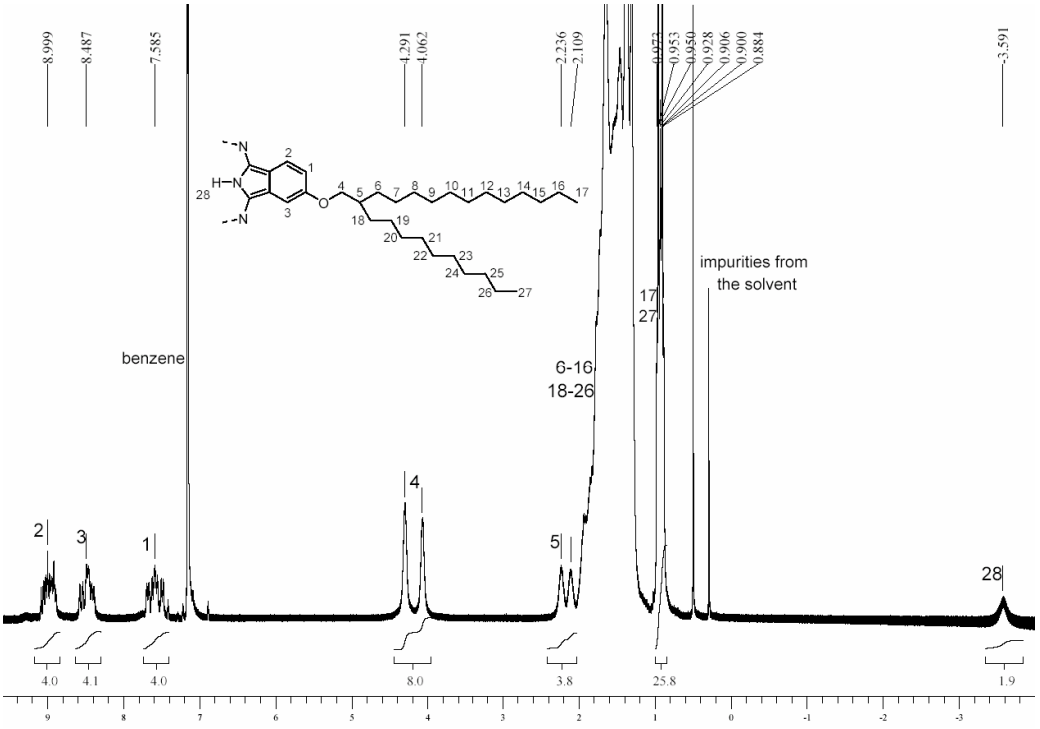

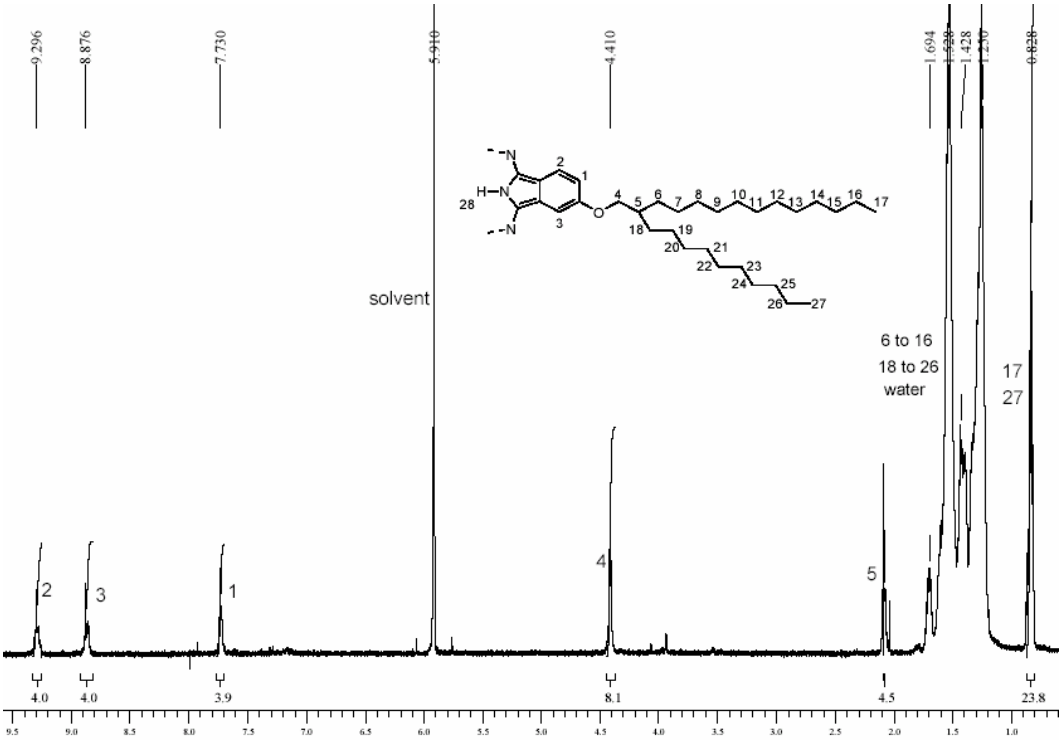

*Figure 2. a) ^{1}H NMR spectrum of **H_2Pc-O-(14,10)$_4$** in C_6D_6 at 25°C b) ^{1}H NMR spectrum of **H_2Pc-O-(14,10)$_4$** in $CDCl_2$-$CDCl_2$ at 100°C.*

The solid-state absorption coefficient was calculated from measurements performed with different film thickness from the following equation:

$\alpha = -\ln (10-A) / d$

where α is the solid state absorption coefficient, A the absordance, and d the thickness of the film. A solid-state absorption coefficient was calculated for each data point; α has an average value of $4.2 \times 104 \pm 0.3 \times 104$ cm-1 at 615 nm.

3. Purification

PCBM was used as received. H2Pc-O-(14,10)4 was purified by chromatography column packed with normal phase silica. Solvents used as mobile phase, i.e. hexane and toluene, were spectrometric grade in order to avoid contamination by solvent impurities. Glassware were cleaned by a KOH/isopropanol mixture and rinsed carefully with distilled water. This procedure allowed for the obtaining of a molecule that was pure as determined by 1H NMR. ICP-OES analysis (in collaboration with AVECIA) did not reveal any traces of inorganic ions or metals, except Si (Table 1).

Table 1. Results of ICP-OES analysis (Inductively Coupled Plasma Optical Emission Spectroscopy)

impurity	Concentration (mg/Kg)	Concentration (atoms/cm^3)	Number atoms/disc
Ag	< 5,0	2,99E+17	8,92E-05
Al	< 10,0	2,39E+18	7,13E-04
As	< 10,0	8,60E+17	2,57E-04
Au	< 5,0	1,64E+17	4,89E-05
B	< 5,0	2,98E+18	8,90E-04
Ba	< 5,0	2,35E+17	7,01E-05
Be	< 5,0	3,58E+18	1,07E-03
Bi	< 10,0	3,08E+17	9,21E-05
Ca	< 10,0	1,61E+18	4,80E-04
Cd	< 5,0	2,87E+17	8,56E-05
Co	< 5,0	5,47E+17	1,63E-04
Cr	< 5,0	6,20E+17	1,85E-04
Cu	< 5,0	5,07E+17	1,51E-04
Fe	< 10,0	1,15E+18	3,45E-04
Hg	< 10,0	3,21E+17	9,60E-05
K	< 10,0	1,65E+18	4,92E-04
La	< 5,0	2,32E+17	6,93E-05
Li	< 5,0	4,64E+18	1,39E-03
Mg	< 5,0	1,33E+18	3,96E-04
Mn	< 5,0	5,87E+17	1,75E-04
Mo	< 5,0	3,36E+17	1,00E-04
Na	< 10,0	2,80E+18	8,37E-04
Ni	< 5,0	5,49E+17	1,64E-04
P	< 25,0	5,20E+18	1,55E-03
Pb	< 10,0	3,11E+17	9,29E-05
Pd	< 5,0	3,03E+17	9,04E-05
Pt	< 10,0	3,30E+17	9,87E-05
Sb	< 5,0	2,65E+17	7,91E-05
Se	< 10,0	8,16E+17	2,44E-04
Si	**80 ±13**	**1,84E+19**	**5,48E-03**
Sn	< 5,0	2,71E+17	8,11E-05
Sr	< 5,0	3,68E+17	1,10E-04
Ti	< 5,0	6,73E+17	2,01E-04
V	< 5,0	6,33E+17	1,89E-04
Zn	< 5,0	4,93E+17	1,47E-04
Zr	< 5,0	3,53E+17	1,06E-04
	< 5,0	1,68E+17	5,01E-05

XPS analysis (in collaboration with Dept. of Physics, IFM Linköping University) revealed that the silicon came from colloidal particles eluted from the silica beads used to pack the columns. This kind of contamination is detrimental neither for the conductivity nor for the processability of the material.

4. Deposition techniques/ Layers sequence

In this project, two main configurations were considered for the active layer: the two-layers geometry and the blended, i.e. bulk heterojunction, geometry. In both cases, the obtaining of an efficient photovoltaic cell is subjected to several requirements: no molecular miscibility between PCBM and H2Pc-O-(14,10)4, homeotropic alignment of

H2Pc-O-(14,10)4 relative to the electrodes, and in the case of blends, a co-continuous morphology.

a) ➔ Bi-layer geometry

The orientation of H2Pc-O-(14,10)4 columns in films was studied by optical microscopy under crossed polarizers. Thick films (between 12 and 20 µm) obtained by deposition of a few mg of phthalocyanine between two glass plates and subsequent heating in the isotropic phase followed by slow cooling displayed homeotropic alignment, as indicated by the dark image and the white linear defaults observed under crossed polarizers. This behaviour was also observed for a large number of other substrates such as ITO, Gold, PEDOT:PSS, poly(isobutylene), fluorinated polymer and PCBM. When the upper plate was removed after annealing, homeotropic alignment was preserved. Subsequent heating in the isotropic phase and slow cooling give, however, a texture characteristic of edge-on alignment, demonstrating by the way that the confinement induced by the upper plate was necessary to induce planar ordering of the phthalocyanine molecules.

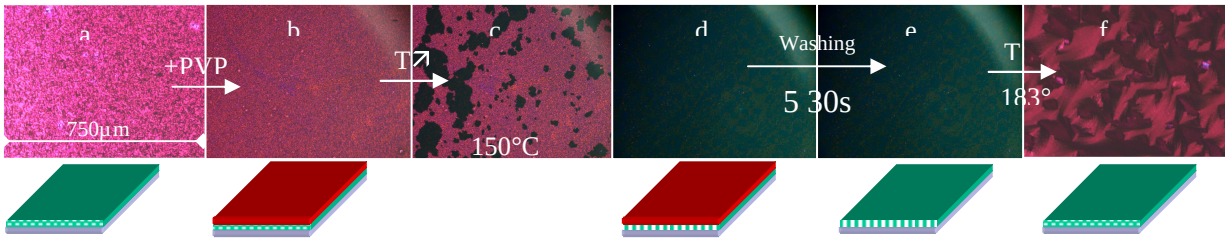

Figure 3: Polarized light microscopy images of a phthalocyanine sample after each step of the process: a) pristine film, b) after PVP spincoating, c) during annealing, transition from disordered to ordered state, d) homeotropically aligned film covered by the polymer layer, e) homeotropically aligned film, after washing, f) disordered film obtained by re-annealing of the washed film.

This was confirm by the results obtained for thin H2Pc-O-(14,10)4 films (up to 300 nm), deposited by spincoating from toluene, heptane or octane solutions. Thermal annealing of those samples lead to edge-on alignment as indicated by the texture observed under crossed polarizers. This thickness range (up to 300 nm) being more suitable for the design of solar cells, the use of a sacrificial confinement layer was considered. The successive steps of the process are illustrated with polarized light microscopy images in figure 2. Since methanol, which is used to dissolve the poly(vinylphenol), is not a solvent for the phthalocyanine, both materials do not mix during spincoating (figure 3a and b) and the removal of the polymer do not damage the liquid crystal layer (figure 3d and e). The development of homeotropic alignment was demonstrated to occur already in the columnar hexagonal phase around 150°C (figure 3c and d). The process is reversible, as

illustrated in figure 2f, since re-annealing of a homeotropically aligned and washed film leads to disordered organization. These results were obtained with H2PC(10.14)4 films thickness from 30 to 300 nm and with polymer films thickness from 470 to 1700 nm.

PCBM could be used as confinement layer, simplifying in a large extend the manufacturing method of the bilayer. Unfortunately, PCBM and H2Pc-O-(14,10)4 are soluble in the same solvents, excluding by the way the spin-coating as the preparation technique of such bi-layer. To overcome this, new PCBM derivatives with fluorinated chain (selectively soluble in fluorinated solvent) or ethylene oxide chains (selectively soluble in water) were synthesized. The synthetic pathways were the following:

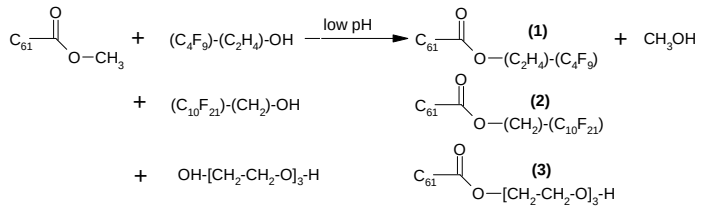

Fluorinated or ethyleneoxide chains where not long enough to induce the solubility of the PCBM derivatives in fluorinated or polar solvents. This option was thus rejected.

In conclusion, the possibility to obtain homeotropically aligned thin films by the use of a polymer sacrificial layer is however the first step toward the obtaining of the bilayer solar cell. It is now necessary to identify an electron conducting materials soluble in solvent that do not dissolve H2Pc-O-(14,10)4.

b) ➔ Bulk heterojunction geometry

Blends of H2Pc-O-(14,10)4 and PCBM in different molar ratio were studied by optical microscopy, DSC, AFM, and X-ray diffraction in order to determine the solubility of PCBM in the liquid crystal and the morphology of the blends.
The phase diagram of the system was determined from the DSC, optical microscopy (Figure 4) and X-ray diffraction measurements (figure 5a,b). As indicated by the decrease of the I to Colh transition temperature as the PCBM content increases, the fullerene derivative is somewhat soluble (a few %) in the liquid crystal derivative. Moreover if sample with a PCBM content up to 5% display phthalocyanine homeotropically aligned, sample with higher PCBM content do not present this properties: PCBM particles are acting as starter for the formation of the new phase, inducing the formation of a large number of domain randomly oriented. Finally, a continuous morphology of the two materials was never observed.

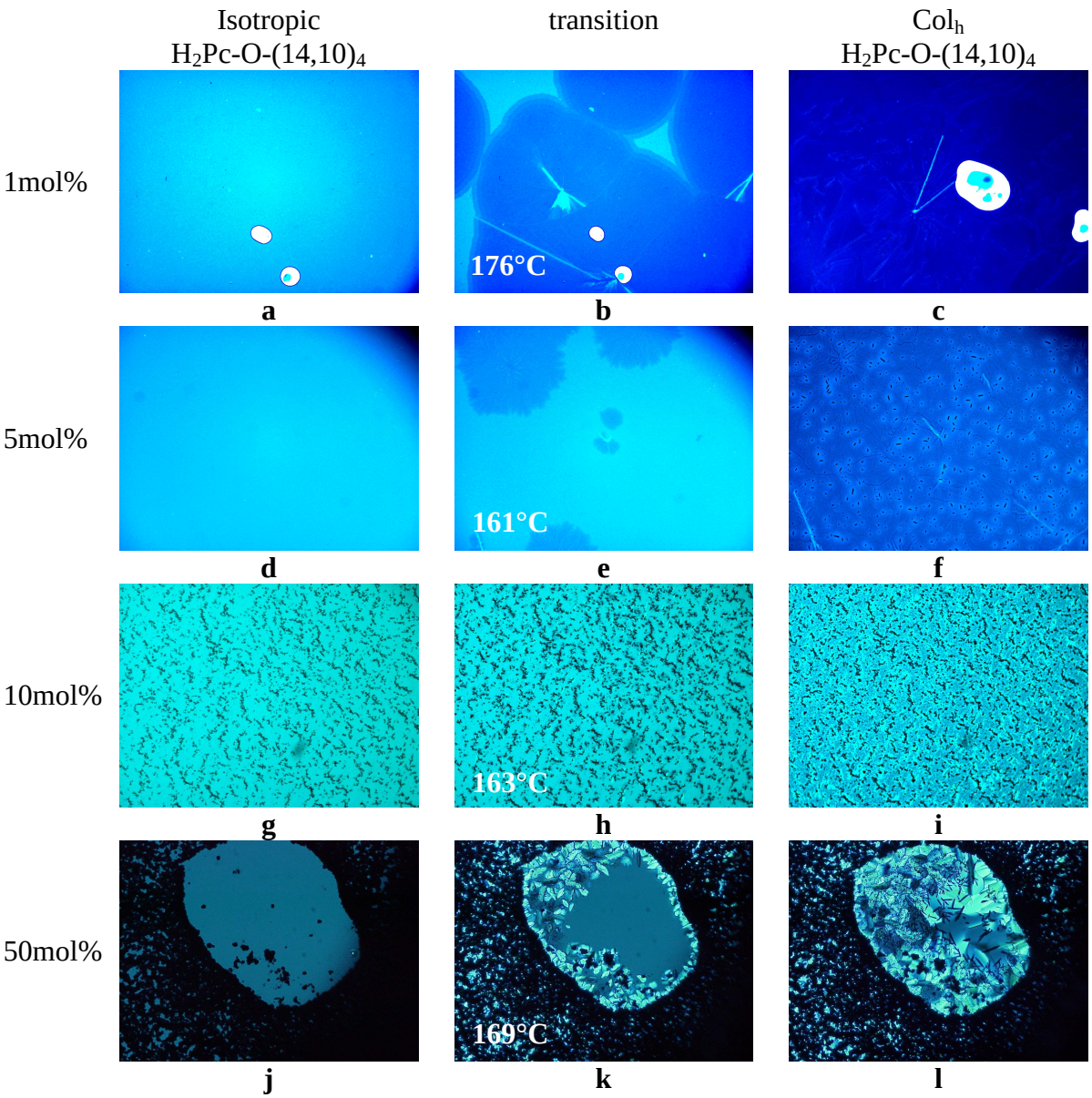

Figure 4. Optical microscopy images of bulk **H_2Pc-O-(14,10)$_4$/PCBM** blends. a, b, c) 1mol%, without polarizers; d, e, f) 5 mol%, without polarizers; g, h, i) 10mol%, under crossed polarizers; j, k, l) 50mol%, under crossed polarizers. a, d, g, j) at 200°C, in the isotropic phase of phthalocyanine; b, e, h, k) at the transition from I to Col_h; c, f, i, l) at 150°C in the Col_h phase of phthalocyanine.

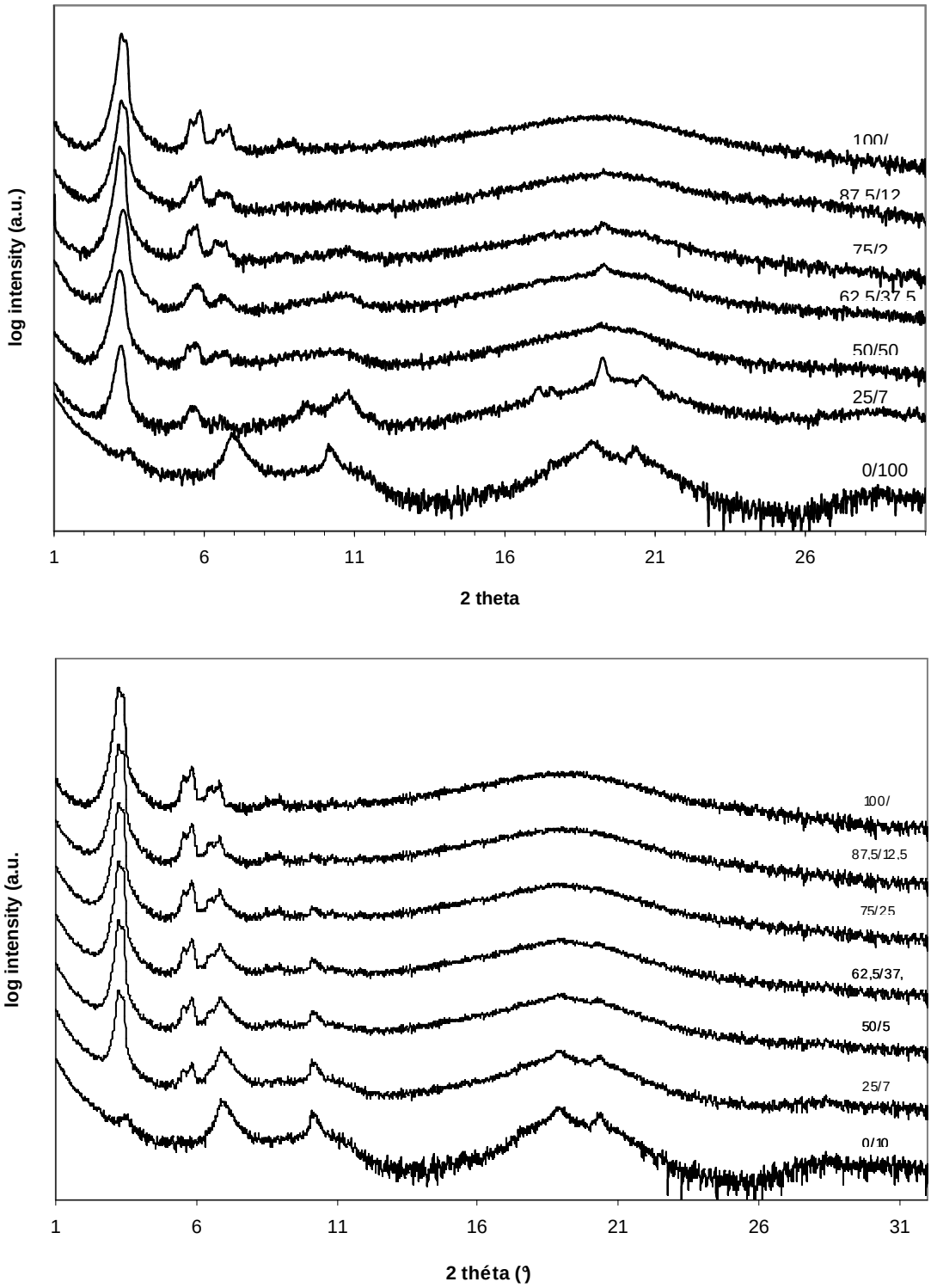

Figure 5. A) X-ray diffractogram of ***H_2Pc-O-(14,10)$_4$/PCBM*** *blends obtained at 25°C. Proportion between the molecules are indicated on the right side of the graph: first diffractrogram at the bottom of the graph is pure* ***PCBM*** *while the last diffractrogram at the top of the graph is* ***H_2Pc-O-(14,10)$_4$****. Peak indexation is*

indicated in brackets. B) Theoritical X-ray diffractogram calculated from the weighed sum of the pure ***H_2Pc-O-(14,10)$_4$*** *and pure* ***PCBM*** *signals in the same proportion as those used experimentally. Proportion between the molecules are indicated on the right side of the graph: first diffractrogram at the bottom of the graph is pure* ***PCBM*** *while the last diffractrogram at the top of the graph is* ***H_2Pc-O-(14,10)$_4$****.*

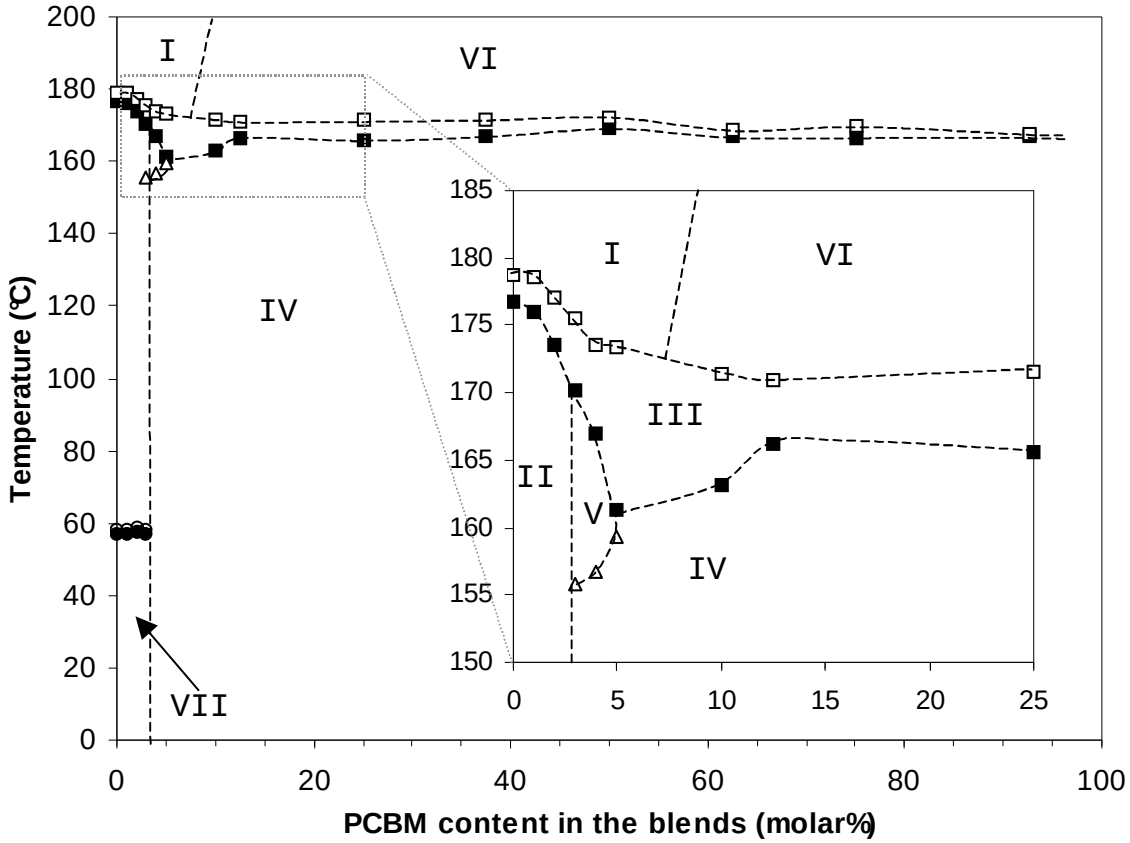

Figure 6*: Phase diagram of the* ***H_2Pc-O-(14,10)$_4$ / PCBM*** *blends as determined by the measurement of the phase transition temperatures by DSC and OM observations under polarized light. □: temperature of the Col$_h$ to I transition; ■: temperature of the I to Col$_h$ transition;* ***O****: temperature of the Col$_r$ to Col$_h$ transition;* ***●****: temperature of the Col$_h$ to Col$_r$ transition; △: temperature at which* ***PCBM*** *segregates from Col$_h$* ***H_2Pc-O-(14,10)$_4$****.* ***I****: isotropic* ***H_2Pc-O-(14,10)$_4$*** *+ dissolved* ***PCBM*** *;* ***II:*** *Col$_h$* ***H_2Pc-O-(14,10)$_4$*** *+ dissolved* ***PCBM; III****: hysteresis region;* ***IV****: Col$_h$* ***H_2Pc-O-(14,10)$_4$*** *+ dissolved* ***PCBM*** *+ solid* ***PCBM****,* ***V****: Col$_h$* ***H_2Pc-O-(14,10)$_4$*** *+ dissolved* ***PCBM****,* ***VI****: isotropic* ***H_2Pc-O-(14,10)$_4$*** *+ dissolved* ***PCBM*** *+ solid* ***PCBM****,* ***VII****: Col$_r$* ***H_2Pc-O-(14,10)$_4$*** *+ dissolved* ***PCBM****.*

In conclusion, bulk heterojunction geometry is thus not a realistic option in the design of solar cell with H2Pc-O-(14,10)4 and PCBM.

D. Partner UNIVERSITE MONS-HAINAUT

1. Introduction

During the SOLTEX project, we have shown that quantum-chemical calculations can provide reliable estimates of the molecular parameters governing the rates of exciton dissociation and charge recombination in donor/acceptor pairs of relevance for organic solar cells. Our approach contrasts with many previous studies in which some of the parameters were calculated and the others extracted from or fitted to experimental data [1-5]. Such a purely theoretical approach allows us establishing guidelines and helping in the design of matching partners and of the most appropriate supramolecular architectures to fabricate highly efficient solar cells; up to now, this design has been mainly performed on an empirical basis.

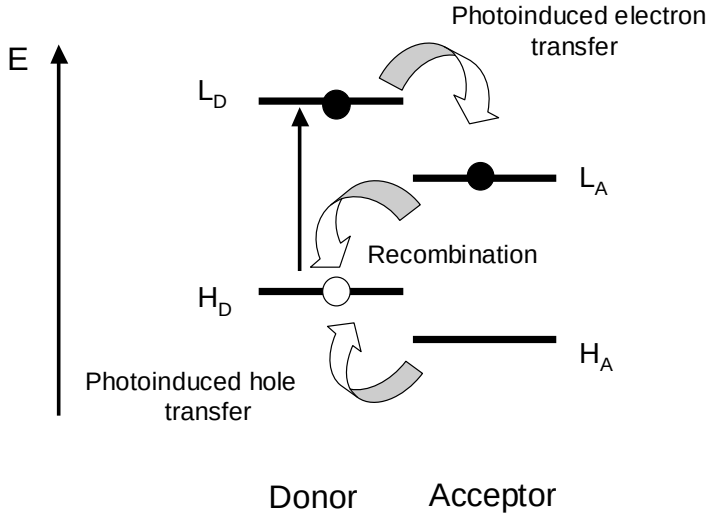

Figure 1: Illustration of the photoinduced electron/hole transfer and charge recombination processes in a donor/acceptor pair (H= HOMO; L= LUMO; D= Donor; A= Acceptor).

The mechanism for light conversion into charges involves four subsequent steps (Figure 1): (i) light is absorbed by the donor and/or the acceptor to generate intramolecular electron-hole pairs; in a simple one-electron picture, an electron is promoted from the HOMO (Highest Occupied Molecular Orbital) level of the excited molecule to its LUMO (Lowest Unoccupied Molecular Orbital) level. These excitations display a binding energy largely exceeding kT, thereby hindering efficient charge generation in single-component devices [6]; (ii) the excitations migrate toward the interface between the donor and the acceptor; (iii) at the interface, when the donor [acceptor] is initially excited, the electron [hole] lying in the LUMO of the donor [HOMO of the acceptor] is transferred to the LUMO of the acceptor [HOMO of the donor] following a photoinduced electron [hole] transfer process; this ultimately yields a charge separated state (with a positive charge on the donor and a negative charge on the acceptor), see Figure 1; (iv) the generated charges

that escape their mutual Coulomb attraction propagate through the organic layer to the electrodes where they are collected.

2. Methodology

Since exciton dissociation and charge recombination both correspond to an electron-transfer reaction, their rates can be estimated in the framework of Marcus theory and extensions thereof [7]. The semi-classical formalism is based on the assumption that the system has to reach the transition state for the transfer to occur; it neglects tunnelling effects that can assist the transfer, especially at low temperatures. These can be treated quantum mechanically by introducing into the rate expression the density of vibrational modes in the initial and final states and their overlap. This is accounted for in the Marcus-Levich-Jortner formalism in which the electron transfer rate writes [8]:

$$k = \left(\frac{4\pi^2}{h}\right) V_{RP}^2 \left(\frac{1}{\sqrt{4\pi\lambda_s kT}}\right) \sum_{\upsilon'} \exp^{-S} \frac{S^{\upsilon'}}{\upsilon'!} \exp\left(\frac{-\left(\Delta G° + \lambda_s + \upsilon' \hbar \langle\omega\rangle\right)^2}{4\lambda_s kT}\right) \qquad \text{Eq. 1}$$

where ΔG° represents the Gibbs free energy of the reaction; VRP is the electronic coupling between the initial and final states and λ the reorganization energy. The latter parameter includes two contributions: (i) the internal part λi which describes the changes in the geometry of the donor and acceptor moieties upon charge transfer [9,10]; and (ii) the external part λs related to the change in electronic and nuclear polarizations of the surrounding medium. In this Equation, a single effective high-frequency mode of energy ħω (that we have set equal to 0.20 eV, that is the typical energy of a carbon-carbon bond stretch in a conjugated system) is treated quantum-mechanically; the low-frequency vibrations (i.e., librations) are treated classically and incorporated into λs. The Huang-Rhys factor S is directly related to the internal reorganization energy (S = λi / ħω) and the summation runs over the vibrational levels in the final state.

a) Gibbs free energy of reaction

ΔG° has been estimated as the energy difference of the constituents in their final and initial states, accounting for the Coulomb attraction between the two charges in the charge-separated state. Thus, for exciton dissociation and when neglecting the entropy contributions, ΔG°dis writes:

$$\Delta G^0_{dis} = E^{D^+} + E^{A^-} - E^{D^*} - E^{A} + \Delta E_{coul} \qquad \text{Eq. 2}$$

$$\text{with} \quad \Delta E_{coul} = \sum_{D+}\sum_{A-} \frac{q_{D+} q_{A-}}{4\pi\varepsilon_0\varepsilon_s r_{D+A-}} - \sum_{D^*}\sum_{A} \frac{q_{D^*} q_A}{4\pi\varepsilon_0\varepsilon_s r_{D^*A}} \qquad \text{Eq. 3}$$

where ED*, ED+, EA, and EA- represent the total energies of the isolated donor in the equilibrium geometry of the lowest excited state and of the cationic state and those of the isolated acceptor in the equilibrium geometry of the ground state and of the anionic state, respectively; qD and qA correspond to the atomic charges on the donor and the acceptor in their relevant state, respectively, that are separated by a distance rDA; □s is the static dielectric constant of the medium. The sums run over all atoms of the two individual molecules. The Gibbs free energy for charge recombination has been estimated from expressions similar to Eqs. 2 and 3 that involve the charge-separated state and the ground state.

In order to compute the first four terms, we have first optimized the geometry of the individual molecules in their various redox states with the help of the Austin Model 1 (AM1) method [11] coupled to a full configuration interaction (FCI) scheme within an active space built from a few frontier electronic levels, as implemented in the AMPAC package [12]. The size of the active space has been chosen in all instances to ensure the convergence of the results. The influence of the dielectric properties of the medium has also been taken into account by means of the COSMO model [13]. The atomic charges of the donor and the acceptor have been obtained from a Mulliken population analysis performed on the AM1-CI/COSMO results.

b) Reorganization energy

The internal part of the reorganization energy λi can be estimated as the average of two quantities λi1 and λi2; in the case of exciton dissociation [14]:

$$\lambda_{i1} = (E^{D^*}(Q_P) + E^{A}(Q_P)) - (E^{D^*}(Q_R) + E^{A}(Q_R)) \qquad \text{Eq .4}$$

$$\lambda_{i2} = (E^{D+}(Q_R) + E^{A-}(Q_R)) - (E^{D+}(Q_P) + E^{A-}(Q_P)) \qquad \text{Eq. 5}$$

where ED*, ED+, EA, and EA- represent the total energy of the isolated donor in the lowest excited state and the cationic state and that of the isolated acceptor in the ground state and the anionic state, respectively; QR and QP refer to the equilibrium geometries of the reactants and products, respectively. All terms have been calculated at the AM1-CI level.

The external part of the reorganization energy λs has been estimated by the classical dielectric continuum model initially developed by Marcus for electron-transfer reactions between ions in solution [15]. The reorganization term is given by:

$$\lambda_s = \frac{1}{8\pi\varepsilon_0}\left(\frac{1}{\varepsilon_{op}} - \frac{1}{\varepsilon_s}\right)\left(\frac{1}{R_D} + \frac{1}{R_A} - 2\sum_D\sum_A \frac{q_D q_A}{r_{DA}}\right) \qquad \text{Eq. 6}$$

where εs is the static dielectric constant of the medium and εop the optical dielectric constant; since the refractive index does not change significantly going from one solvent to another, we have set εop equal to a typical value of 2.25 [16,17]. The qD and qA terms denote the atomic charges on the ions, as estimated at the AM1/CI-COSMO level, that have been introduced in Marcus expression to account for the molecular topologies of the donor and acceptor units. RD and RA are the effective radii of the donor and acceptor, respectively, that are estimated as the radius of the sphere having the same surface as the surface accessible area of the molecule provided by COSMO.

c) Electronic coupling

The electronic coupling VRP appearing in Eq. 2 has in principle to be evaluated in a diabatic description (where the initial and final states do not interact) as half the splitting at the transition state geometry. Since the excited states of the systems are described here by means of a configuration interaction (CI) scheme, we actually do take into account the interaction between the two states and hence provide an adiabatic description of the system. In that case, VRP can be estimated from quantities given directly by the CI calculations (or by experiment) in the framework of the Generalized Mulliken-Hush (GMH) formalism which refers to a vertical transition from the initial to the final state [18,19]. In a two-state model, VRP writes:

$$V_{RP} = \frac{\mu_{RP}\,\Delta E_{RP}}{\sqrt{(\Delta\mu_{RP})^2 + 4(\mu_{RP})^2}} \qquad \text{Eq. 7}$$

where ΔERP corresponds to the energy difference, ΔμRP to the dipole moment difference, and μRP to the transition dipole moment between the initial and final states (projected in all cases along the ΔμRP direction mostly orientated along the stacking axis [20]). These parameters have been evaluated using the semiempirical Hartree-Fock INDO (Intermediate Neglect of Differential Overlap) method [21] coupled to a single configuration interaction scheme (SCI). The full details of our methodology are given in Ref. 22.

3. Results and discussion: Phthalocyanine as donor and perylenebisimide as acceptor

We have first applied our approach to a donor-acceptor complex built from a free-base phthalocyanine (Pc) as the donor and perylene bisimide (PTCDI) as the acceptor (see the chemical structures in Figure 2). The choice of these conjugated molecules is motivated by the fact that the electronic and optical properties of blends made of Pc and PTCDI derivatives have been the focus of many experimental studies [23-28]. Pc molecules are low-energy absorbers, with the lowest absorption band peaking around 1.8 eV [29]; this closely matches the spectral region where solar emission is most intense. Moreover, Pc

molecules have been shown to be excellent candidates for charge and exciton transport [30].

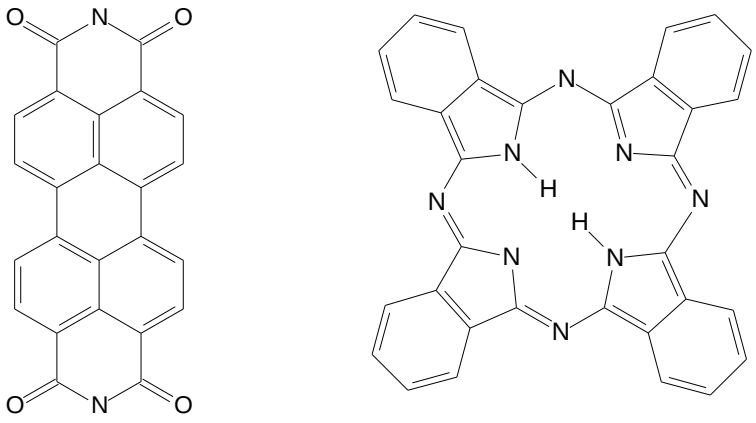

Figure 2: Chemical structures of phthalocyanine (Pc, right) and of perylenebismide (PTCDI, right).

With Pc initially photoexcited in a cofacial complex with the intermolecular distance fixed at 4 Å, we obtain values of 3.6 x 1013 s-1 and 5.4 x 1013 s-1 for the exciton dissociation rate for εs = 3 and 5, respectively. Note that there are actually two dissociation pathways due to the fact that the LUMO and LUMO+1 levels of a Pc molecule are quasi-degenerate. The exciton dissociation process occurs in the normal region of Marcus since $|\Delta G°| < \lambda$ (-0.23 eV versus 0.52 eV). The transfer rate would increase significantly if $|\Delta G°|$ and λ were to converge towards a similar value; this does not occur here since the absolute values of $\Delta G°$dis and λ both increase with medium polarity. For the same geometry, we estimate recombination rates of 1.7 x 102 s-1 and 2.7 x 104 s-1 for εs = 3 and 5, respectively. The extreme slowness of this process originates from the vanishingly small electronic couplings (as a result of symmetry constraints linked to the shape of the orbitals of the involved electronic levels [22]) and from the fact that recombination occurs deep into the inverted region of Marcus ($|\Delta G°| = 1.65$ eV >> $\lambda = 0.45$ eV for εs = 3). Charge recombination gets faster when the dielectric constant is increased due to the opposite evolutions of $\Delta G°$rec and λs, which tends to reduce the gap between their absolute values.

If we assume that the acceptor is initially excited, we calculate exciton dissociation rates of 1.1 x 1010 and 2.7 x 1011 s-1 for εs = 3 and 5, respectively. This translates into a ratio kD/kA (where kD [kA] corresponds to the rate when the donor [acceptor] is initially excited, respectively) of 3333 and 204 for εs = 3 and 5. The reduction in the exciton dissociation rate when exciting the acceptor is associated with the increase in energy gap between $|\Delta G°|$ and λ, the dissociation actually taking place in the inverted region. Thus, the nature of the excited species also plays a significant role in the dynamics of charge generation in solar cells.

a) Influence of structural disorder

We have analyzed the evolution of the electronic coupling associated to the two dissociation pathways for exciton dissociation when Pc is initially excited and to charge recombination when rotating one molecule around the "stacking" axis for a static dielectric constant of 3. Interestingly, we find that there always exists an efficient pathway for exciton dissociation whatever the rotational angle and that the nature of the dominant pathway reverses in going from 0 to 90° (Figure 3); this is explained by the fact that the lowest two unoccupied orbitals of Pc are polarized in perpendicular directions. The calculated couplings reflect a fine balance between the relative positions of the two molecules and the shape of the revelant wavefunctions [31].

The dimensionality of the Pc molecule thus appears to be a key parameter that contributes to high efficiencies in organic solar cells by creating a quasi degeneracy of electronic levels and in turn a strong insensitivity to rotational disorder; such a behavior is not expected when mixing two rod-like molecules. The charge recombination rate is weakly affected by the rotational angle due to the fact that the HOMO level of Pc is fully delocalized over the conjugated core.

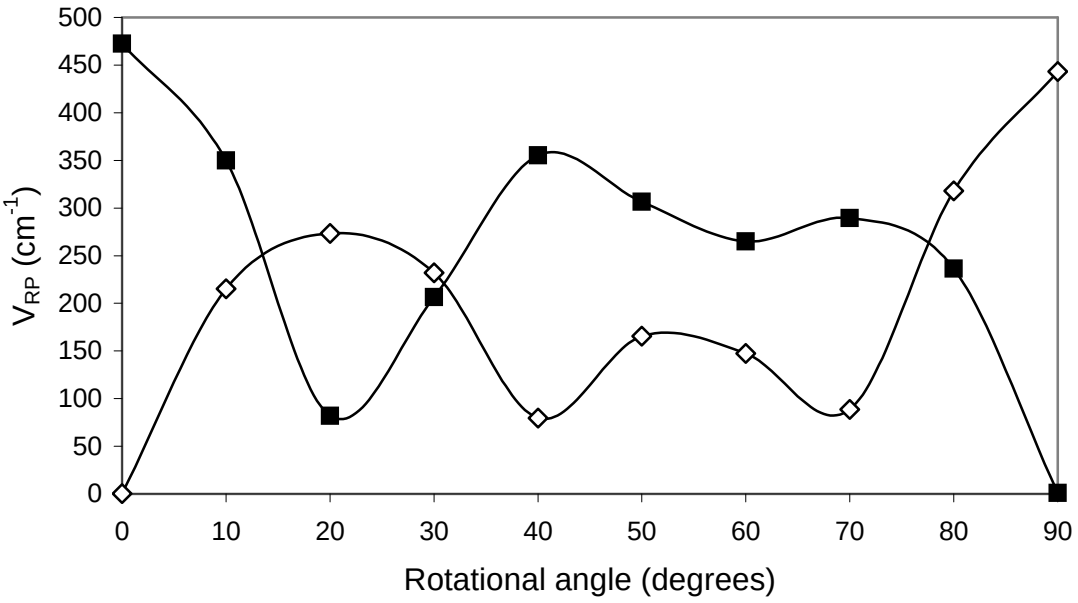

Figure 3: Evolution of the INDO/SCI-calculated electronic coupling of the two different pathways for exciton dissociation in the Pc/PTCDI complex (with the two molecules separated by 4 Å) when rotating the PTCDI molecule around the stacking axis; the zero value corresponds to the cofacial geometry.

4. Results and discussion: three-ring phenylenevinylene oligomer as donor and perylenebisimide as acceptor

Our approach has been next applied to model complexes involving a three-ring phenylenevinylene oligomer (PPV3) as donor and a perylenebisimide molecule (PTCDI) as acceptor (see chemical structures in Figure 4). This study is motivated by the fact that several model systems based on PPV-related segments and perylenebisimide derivatives have been recently synthesized, in particular by TUE, to shed light into the dynamics of charge generation and recombination processes [32-34].

We have first considered a cofacial dimer built by superimposing the centers of mass of the PPV oligomer (assumed to be fully planar) and perylene, with their molecular axes lying parallel to one another and the intermolecular separation set at 4 Å (Figure 4). We collect in Figure 4 the energy of the relevant excited states of the dimer in their fully relaxed geometries (DA, D*A, DA* and D+A-), as calculated at the AM1-CI/COSMO level. The lowest excited state of the three-ring PPV oligomer is estimated to lie at 3.84 eV above the ground state, which is 0.3-0.4 eV higher than the experimental value in solution [35]; similary, the lowest electronic excitation of perylene is calculated at 2.8 eV to be compared to the experimental value of ~ 2.5 eV [36]. In both cases, the excited state is mostly described by an electronic excitation between the HOMO and LUMO levels of the molecule. In the cofacial geometry, the lowest charge-transfer excited state is found to be almost isoenergetic with the lowest intramolecular excited state of PTCDI (assuming a static dielectric constant of 3.5). This results into a driving force of –1.0 eV and + 0.03 eV for the photoinduced electron and hole transfer process, respectively. The energy difference between the ground state and the lowest charge-transfer excited state (i.e., the driving force $\Delta G°$ for the charge recombination process) is estimated to be -2.84 eV; this value should be seen as an upper limit in view of the previous considerations. Interestingly, the calculations point to the existence of a second charge-transfer excited state lying 1.15 eV above the lowest charge-transfer state.

For the charge recombination process, we can safely assume that it originates entirely from CT1 owing to the large energy difference between the lowest two charge-transfer excited states. The charge recombination process globally results from the transfer of one electron from the LUMO of the acceptor to the HOMO of the donor.

We can estimate the transfer rates of the various electronic processes in the model complex by injecting the different molecular parameters ($\Delta G°$, λi, λs, VRP) in Eq. 1. Doing so, we obtain values of 1.31 x 105 and 9.12 x 109 s-1 for the photoinduced electron transfer involving CT1 and CT2 (the same λi and λs values are assumed for the two states), respectively, 5.91 x 106 s-1 for the photoinduced hole transfer, and 1.89 x 108 s-1 for the charge recombination. The photoinduced electron transfer via CT1 and the charge recombination processes occur in the inverted Marcus region ($|\Delta G°|>\lambda$) while the other two processes take place in the normal region ($|\Delta G°|<\lambda$). The most efficient processes are the charge recombination and the photoinduced electron transfer via CT2,

i.e., those for which the electronic coupling has a significant value. The magnitude of the electronic coupling is driven once again by the symmetry of the electronic levels involved in a given process [37].

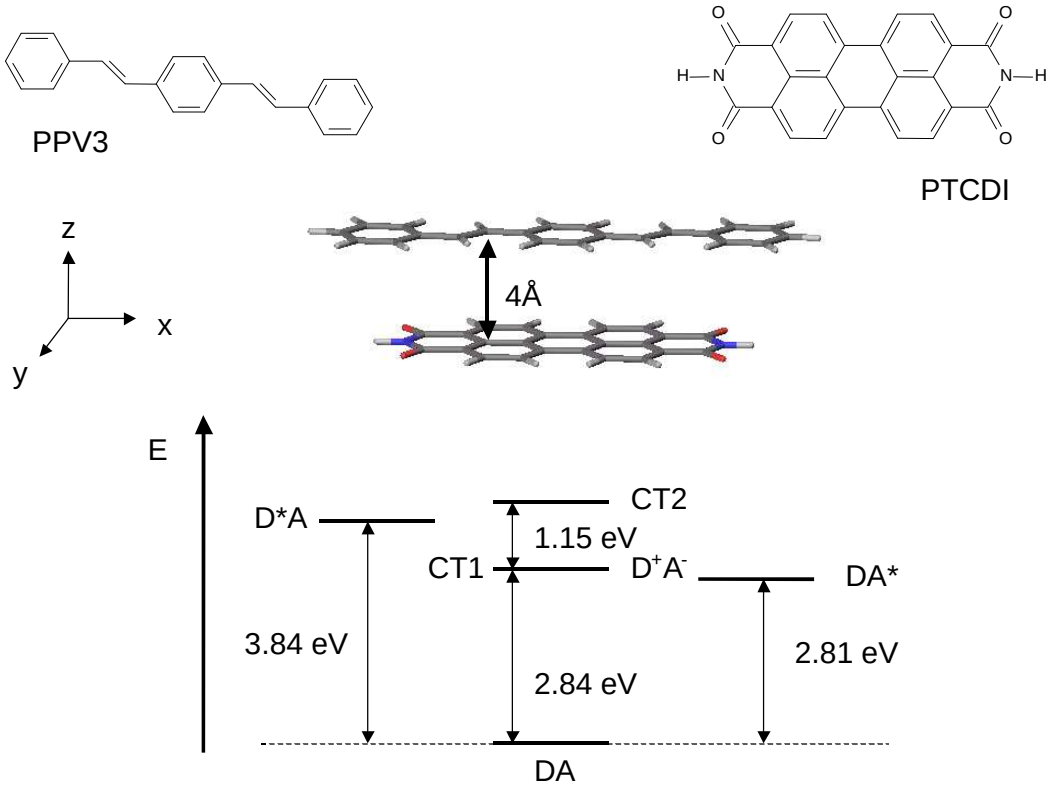

Figure 4: Energy diagram of the relevant states in a cofacial dimer built from one three-ring PPV oligomer as donor and one perylenebisimide molecule as acceptor, with an intermolecular distance fixed at 4 Å. The chemical structures of the two compounds are also shown.

That an excited charge-transfer state has to be invoked to rationalize the full dynamics of exciton dissociation is consistent with recent experimental data collected by Janssen and co-workers for tryad systems where two four-ring PPV oligomers are covalently attached to the terminal ends of a perylene derivative [38]. In this study, an energy transfer initially takes place from the PPV segment to the perylene and is followed by a photoinduced hole transfer via two dissociation pathways.

5. Role of bridging units

So far, we have considered complexes in which the donor and acceptor units are superimposed. In such arrangements, the exciton dissociation is generally larger than the typical decay rate of the excitations, as required for organic solar cells. When the donor and acceptor units are lying in the same plane, the transfer rate appears to be much too

slow to compete with decay processes. This has motivated the study of model systems in which the donor and acceptor are connected covalently by a bridge. To do so, we have considered a system where a donor molecule (a pentacene molecule) is connected to an acceptor (a pentacene molecule substituted by four cyano groups) by means of a saturated bridge into two different conformations; in the first one, the carbon atoms of the bridge are lying in the plane of the pentacene molecules while they adopt a stair-like geometry in the second configuration. Figure 7 describes the evolution of the exciton dissociation rates as a function of the distance between the donor and acceptor units without a bridging unit and with the bridge in the two conformations that we have considered. Strikingly, the rate is significantly increased in the presence of the bridge and is larger for the stair-case geometry; the latter allows for efficient long-range charge transfer between the donor and acceptor units. This evolution is explained by the fact that the frontier electronic levels of the pentacene molecules get delocalized over the bridge; this effect is more pronounced for the stair-case geometry since the σ-bonds of the saturated chains are parallel to the π-orbitals of the pentacene molecules, thus promoting stronger interactions (see Figure 8).

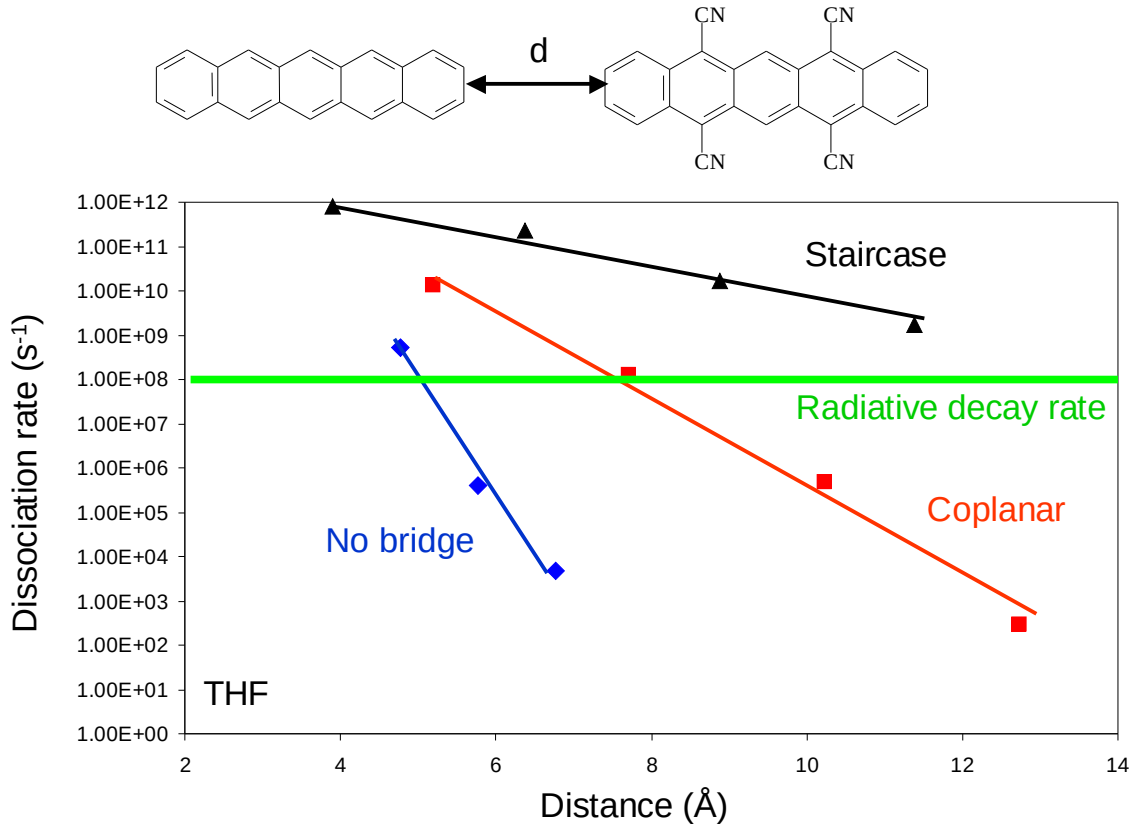

Figure 7 : Evolution of the exciton dissociation rates as a function of the distance between the donor and acceptor without a bridging unit and with a bridge adopting the two conformations that we have considered. The chemical structures of the donor and acceptor are reported on top.

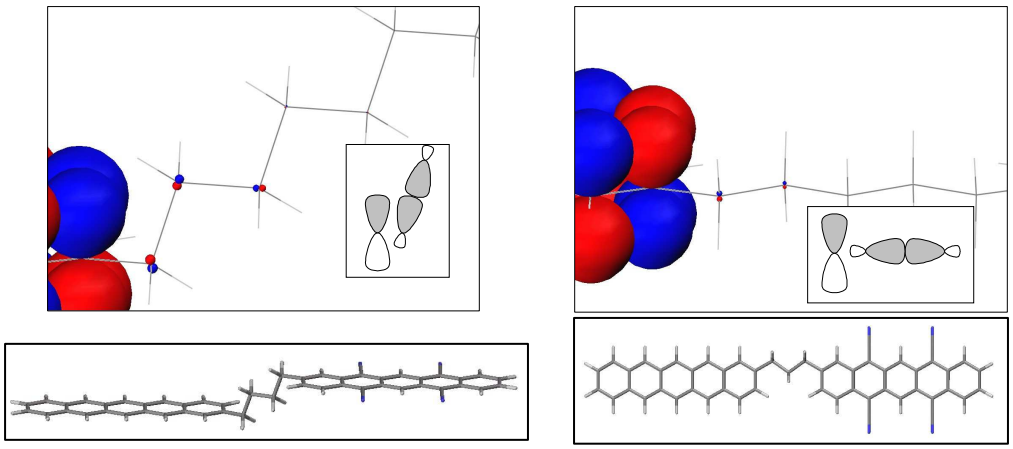

Figure 8 : Ilustration of the delocalization of the π-orbitals of the pentacene molecules over the bridge for the stair-case (left) and coplanar (right) conformation.

The calculations thus demonstrate that linking covalently the donor and acceptor units allows for efficient charge transfer between two molecules lying in the same plane. This cannot be achieved without a bridging unit. Long-range charge transfer assisted by a bridge also contributes in reducing the Coulomb attraction between the photogenerated charges and thus favor their separation to create free carriers.

6. Summary

We have developed an original theoretical approach to estimate all molecular parameters entering into the rates of exciton dissociation and charge recombination in model donor/acceptor pairs that can be used for solar cell applications. For sake of illustration, this approach has been applied to complexes made of a phthalocyanine molecule or a three-ring PPV oligomer as the donor and a perylene molecule as the acceptor.

The results point to the role of several factors in defining the rates of the two processes:
(i) the relative positions of the interacting molecules, which dictates the extent of spatial overlap between the electronic wavefunctions;
(ii) the symmetry of the relevant electronic levels that can be exploited to strongly limit the detrimental charge recombination process;
(iii) the dimensionality of the molecules; the two-dimensional character of the phthalocyanine molecule introduces a quasi degeneracy in the electronic levels and by extension a high insensitivity to rotational disorder; this might rationalize the reason for which the most efficient solar cells to date incorporate derivatives of the three-dimensional C60 molecule that is characterized by the presence of several quasi-degenerate frontier electronic levels.

The calculations have also demonstrated that, in some instances, a dissociation pathway involving an excited charge-transfer state has to be taken into account to fully rationalize the dynamics of the charge generation process; by extension, the number of charge-transfer states to be considered is expected to grow with the molecular size of the donor and/or acceptor. We believe that, in close collaboration with synthetic works and device characterizations, our approach paves the way towards the establishment of general guidelines to determine the best matching partners and the best supramolecular architectures for the development of highly efficient organic solar cells.

(1) References

[1] Pourtois, P.; Beljonne, D.; Cornil, J. ; Ratner, M.A. ; Brédas, J.L. J. Am. Chem. Soc. 2002, 124, 4436.
[2] Clayton, A.H.A.; Ghiggino, K.P.; Wilson, G.J.; Paddon-Row, M.N. J. Phys. Chem. 1993, 97, 7962.
[3] Filatov, I.; Larsson, S. Chem. Phys. 2002, 284, 575.
[4] Redmore, N.P.; Rubtsov, I.V.; Therien, M.J. J. Am. Chem. Soc. 2003, 125, 8769.
[5] Weiss, E.A.; Ahrens, M.J.; Sinks, L.E.; Gusev, A.V.; Ratner, M.A.; Wasielewski, M.R. J. Am. Chem. Soc. 2004, 126, 5577.
[6] Brabec, C. J.; Sariciftci, N. S.; Hummelen, J. C. AdV. Funct. Mater.2001, 11, 15.
[7] Marcus, R.A. Rev. Mod. Phys. 1993, 65, 599.
[8] Electron Transfer: From Isolated Molecules to Biomolecules, Adv. Chem. Phys.; Bixon, M; Jortner, J. Eds.; Wiley, New York, 1999, Vols 106-107.
[9] Sakanoue, K.; Motoda, M.; Sugimoto, M.; Sakaki, S. J. Phys. Chem. A 1999, 103, 5551.
[10] Coropceanu, V; Malagoli, M.; da Silva Filho, D.A.; Gruhn, N.E.; Bill, T.G.; Brédas, J.L. Phys. Rev. Lett. 2002, 89, 275503.
[11] Dewar, M.J.S.; Zoebisch, E.G.; Healy, E.F.; Stewart, J.J.P. J. Am. Chem. Soc. 1985, 107, 3902.
[12] Ampac 6.55, created by Semichem Inc., 7128 Summit, Shawnee, KS 66216, USA 1997.
[13] Klamt, A.; Schürmann, G. J. Chem. Soc., Perkin Trans. 1993, 2, 799.
[14] Cornil J.; Beljonne, D.; Coropceanu, V.; Brédas, J.L., Chem. Rev. 2004, 104, 4971.
[15] Marcus, R.A. J. Chem. Phys. 1965, 43, 679.
[16] Handbook of Chemistry and Physics, 76th edition, Lide, R.D.; Frederikse, H.P.R. CRC Press, 1995.
[17] Madigan, C.F.; Bulovic, V. Phys. Rev. Lett. 2003, 91, 247403.
[18] Cave, R.J.; Newton, M.D.; Chem. Phys. Lett. 1996, 249, 15
[19] Cave, R.J.; Newton, M.D. J. Chem. Phys. 1997, 106, 9213.
[20] Nelsen, S.F.; Newton, M.D. J. Phys. Chem. A 2000, 104, 10023.
[21] Ridley, J.; Zerner, M.C. Theoret. Chim. Acta 1973, 32, 111.
[22] V. Lemaur, M.C. Steel, D. Beljonne, J.L. Brédas, and J. Cornil. J. Am. Chem. Soc. 2005, 127, 6077.
[23] Tang, C.W. Appl. Phys. Lett. 1986, 48, 183.
[24] Wöhrle, D.; Meissner, D. Adv. Mater. 1991, 3, 129.

[25] Adams, D.M.; Kerimo, J.; Olson, E.J.C.; Zaban, A.; Gregg, B.A.; Barbara, P.F. J. Am. Chem. Soc. 1987, 119, 10608.
[26] Lane, P.A.; Rostalski, J.; Giebeler, C.; Martin, S.J.; Bradley, D.D.C.; Meissner, D. Sol. Energ. Mat. Sol. C 2000, 63, 3.
[27] Hiromitsu, I.; Murakami, Y.; Ito, T. J. Appl. Phys. 2003, 94, 2434.
[28] Aroca, R.; Del Cano, T.; de Saja, J.A. Chem. Mater. 2003, 15, 38.
[29] Edwards, L.; Gouterman, M. J. Mol. Spectrosc. 1979, 33, 292.
[30] J. Tant, Y.H. Geerts, M. Lehmann, V. De Cupere, G. Zucchi, B.W. Laursen, T. Björnholm, V. Lemaur, V. Marcq, A. Burquel, E. Hennebicq, F. Gardebien, P. Viville, D. Beljonne, R. Lazzaroni, and J. Cornil. J. Phys. Chem. B 2005, 109, 20315.
[31] Lemaur, V.; da Silva Filho, D.A.; Coropceanu, V.; Lehmann, M.; Geerts, Y.; Piris, J.; Debije, M.G.; van de Craats, A.M.; Senthilkumar, K.; Siebbeles, L.D.A.; Warman, J.M.; Brédas, J.L.; Cornil, J., J. Am. Chem. Soc. 2004, 126, 3271.
[32] Neuteboom, E.E.; vanHal, P.A.; Janssen, R.A.J. Chem. Eur. J. 2004, 10, 3907.
[33] Würthner, F.; Chen, Z.; Hoeben, F.J.M.; Osswald, P.; You, C.C.; Jonkheijm, P.; Herrikhuyzen, J.V.; Schenning, A.P.H.J.; van der Schoot, P.P.A.M.; Meijer, E.W.; Beckers, E.H.A.; Meskers, S.C.J.; Janssen, R.A.J. J. Am. Chem. Soc. 2004, 126, 10611.
[34] Neuteboom, E.E.; Meskers, S.C.J.; van Hal, P.A.; van Duren, J.K.J.; Meijer, E.W.; Janssen, R.A.J.; Dupin, H.; Pourtois, G.; Cornil, J.; Lazzaroni, R.; Brédas, J.L.; Beljonne, D. J. Am. Chem. Soc. 2003, 125, 8625.
[35] Schenk, R.; Gregorius, H.; Müllen, K. Adv. Mater. 1991, 3, 492.
[36] Offermans, T.; Meskers, S.C.J.; Janssen, R.A.J. J. Chem. Phys. 2003, 119, 10924.
[37] Burquel, V. Lemaur, D. Beljonne, R. Lazzaroni, and J. Cornil. J. Phys. Chem. A 2006, 110, 3447.
[38] Beckers, E.H.A.; Meskers, S.C.J.; Schenning, A.P.H.J.; Chen, Z.; Würthner, F.; Janssen, R.A.J. J. Phys. Chem. B 2004, 108, 6933.

E. Partner UNIVERSITEIT HASSELT

1. Introduction.

The main contribution of UHasselt to the TAP-project "SOLTEX" relates to the synthesis of active materials for plastic solar cells. These organic materials are essentially of the class of so called Low Band Gap Polymers, which show on the one hand p-type behavior and on the other hand have an absorption in the visible shifted to the red part of the spectrum. The main interest in the context of the project is to achieve in this way a better matching of the absorption spectrum of the material and the emission spectrum of the sun. UHasselt has many years of experience in design and development of synthetic routes toward this class of conjugated polymers. This expertise has been put to use in the project and further development to improved materials was pursued.
In a second priority the use of p-type conjugated polymers were explore which show increased polarity. This may lead to improved solubility in environmentally acceptable solvents and progress in this field may have important impact on the implementation of polymeric solar cells in technological viable applications. It was expected that experiences obtained with polar, in this case, Poly(p-Phenylene Vinylene) derivatives, in solar cells may give relevant input toward the development of optimized Low Band Gap (LBG) polymers. A third, more minor activity, started in the last year of the project, relates to an exploration of potential n-type conjugated polymers. It is clear also from the work of ULB toward p- and n-type semiconductors, that there is a need from a technological point of view for alternative n-type materials to possibly replace C60 derivatives. In function of economics and stability of the bulk-heterojunction morphology, the use of n-type conjugated polymers may lead to strongly improved characteristics of solar cells. However said materials are virtually unexplored in literature. There is still some room for new concepts of which we explored one possibility, e.g. Poly(Fluoranthene Vinylene) (PFV) derivatives.

2. Synthesis and characterization of LBG p-type conjugated polymers.

Low band gap systems which have been explored by UHasselt since 1988 cover a broad range of structures, e.g. Poly(IsoThiaNaphthene) (PITN) derivatives as structures A and B and 4-Dicyanomethylene-4H-cyclopenta[2,1-b;3,4-b']dithiophene derivatives C (Figure 1). The former were abandoned because of the tedious chemistry that was needed to synthesize them. More particular, it was established that it was difficult to obtain high enough molecular weights for the polymer and for most derivatives the pathway toward monomer synthesis showed to be quite long. The chemistry behind the latter systems promised to yield in an efficient convergent synthesis strategy the envisaged materials, but it was demonstrated that this class of materials systematically showed low mobility's for charge carriers ($\mu fe < 10\text{-}6$ cm2/Vs), and this although initial solar cell device characteristics were quite promising: Voc = 360 mV, Jsc =0.62 mA/cm2 and a FF = 45%

yielding an efficiency of 0.14%. As mobility showed to be low no excellent performance of these materials in optimized photovoltaic devices could be expected and thus the use of these LBG materials was not longer considered in the project after the first year.

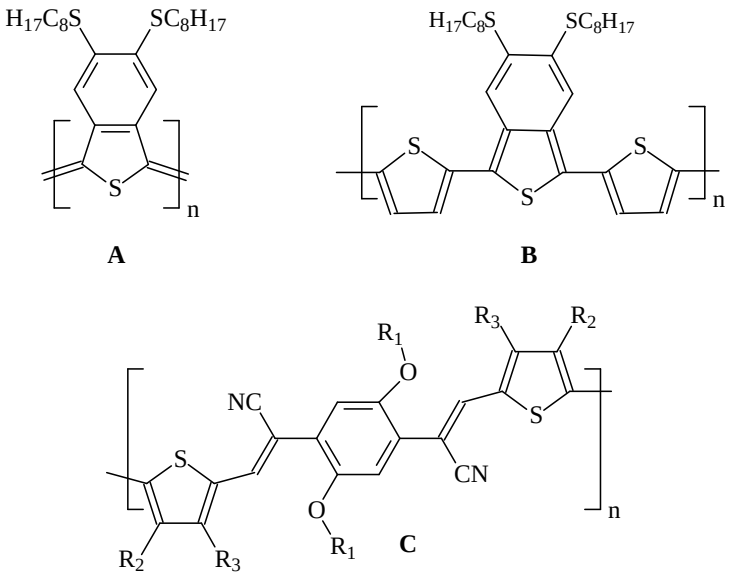

Figure 1: Low Band Gap structures

A second approach to low band gap conjugated polymers builds further on the class of simple Poly(3HexylThiophene) (P3HT) type of derivatives. These conjugated polymers show high performances due to there high mobility for charge carriers and the red shifted absorption (Eg = 1.9 eV) compared to for example MDMO-PPV (Eg = 2.2 eV). Recently it was claimed by Heeger et al. (Adv.Func.Mater. 2005, 1617), that a 5% efficiency in solar cells is within reach. IMEC demonstrated within the SOLTEX-project a quite similar value for the efficiency. Irrespectively of the state of the art of these materials, a further shift of the absorption spectrum toward longer wavelength can be envisaged by moving toward the development of Poly(2,5-Thienylene Vinylene) (PTV) derivatives (Figure 2). From former work in our group it could be expected that for PTV derivatives compared to PT's, a similar mobility of charge carriers can be obtained.

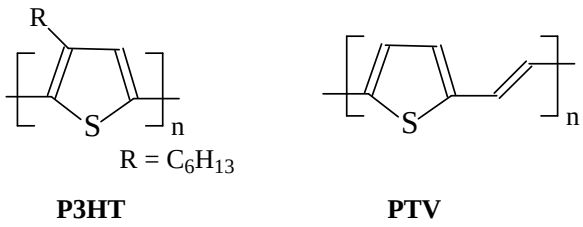

Figure 2: PT and PTV structures

Secondly as a result of a continuous effort in the UHasselt since 1999 to explore synthetic routes toward PTV's, it was found within the PhD work of Anja Henckens that PTV's are

synthetically accessible via dithiocarbamate monomers in strongly basic conditions. This work was taken along from the start of the project. The general scheme associated with this dithiocarbamate route is depicted in Figure 3. Initially as a base LiDiïsopropylAmide (LDA) was use to convert the starting product to the intermediate Quinodimethane derivative, which is the actual monomer in this type of polymerizations. The precursor polymer formed can then be converted to the conjugated polymer by heating in film or in solution, e.g. refluxing o-dichlorobenzene.

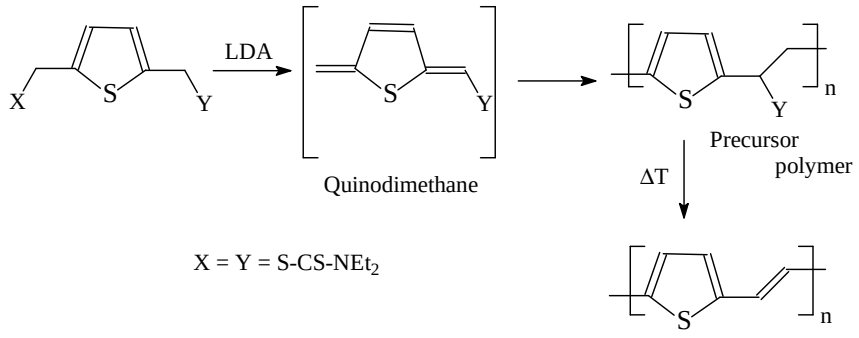

Figure 3: The Dithiocarbamate route towards PTV derivatives

A first series of PTV derivatives that were synthesized via this new route consisted of poly(3,4- diphenyl-2,5-Thienylene Vinylene) derivatives (Figure 4). The corresponding monomers were obtained via reaction of the dichloride derivatives in excellent yield (> 90%). Polymerization was performed in THF with LDA as a base under inert and dry conditions. Reasonable yields were obtained for as well the materials with R = H (entry 1 and 2) and R = n-Butyl (entry 3, Table 1). The molecular weight was sufficiently high to observe good film forming properties of the precursor polymer. It was observed that the material with n-Butyl side chains was also soluble after conversion of the precursor polymer in common organic solvents, like Chloroform and THF.

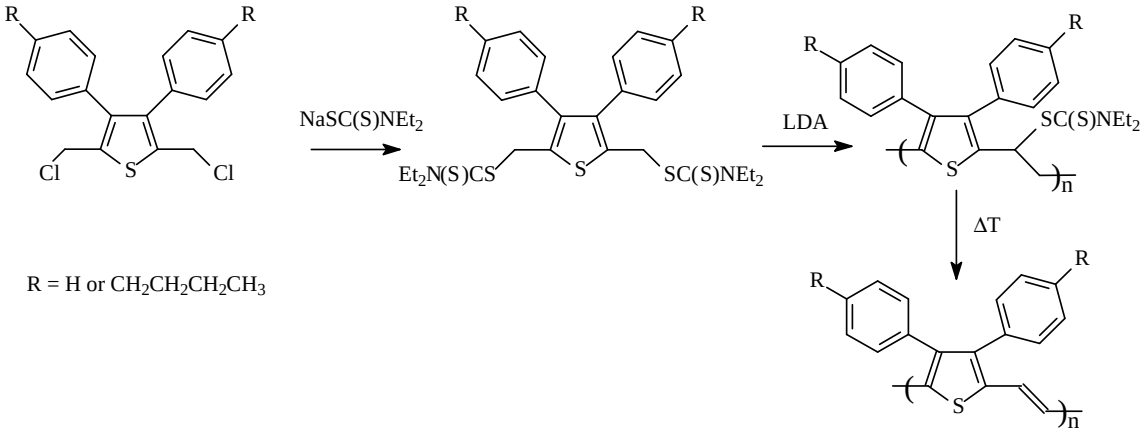

Figure 4: Poly(3,4- diphenyl-2,5-Thienylene Vinylene) derivatives via the dithiocarbamate route

Entry	**Polymerization temperature**	**Yield (%)**	**M_w (x 10^{-3})**	**PD**
1	**0℃**	**20**	**50.4**	**1.4**
2	**-78℃**	**40**	**29.8**	**1.2**
3	**-78℃ → 0℃**	**35**	**24.6**	**1.2**

Table 1: Polymerization results toward poly(3,4- diphenyl-2,5-Thienylene Vinylene) derivatives.

These materials were fully characterised by spectroscopic techniques as NMR, FT-IR and UV-Vis. In situ UV/vis and in situ FT-IR measurements indicate a conversion temperature of 115°C as observed before and a stability of the conjugated system beyond 300°C under inert atmosphere for R = H and until a temperature of 275°C for R = Bu (Figure 5).

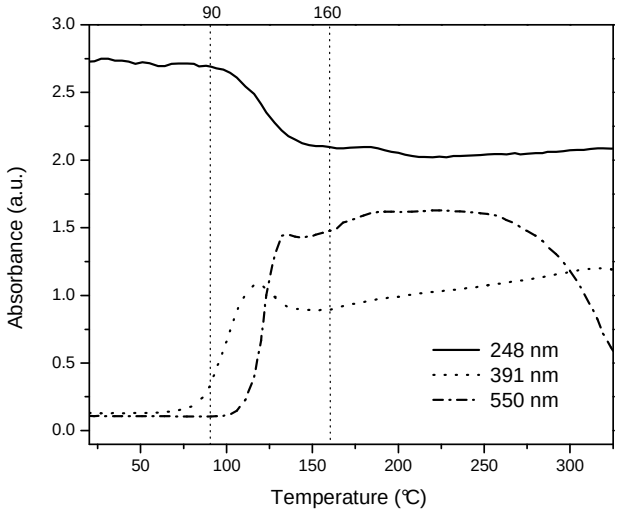

Figure 5: In situ UV/vis of 3,4-diphenyl-PTV with R = Bu

The absorption characteristics in UV/vis revealed a lambda max of 590 nm for both polymers and an optical band gap of about 1.7 eV, which is consistent with a LBG polymer. Using cyclic voltammetry stability of the oxidised and reduced state was evaluated and an estimate of HOMO and LUMO levels was performed (-4.92 eV and -3.11 eV respectively). The cyclic voltammograms of both conjugated polymers display distinct oxidation and reduction processes (Figure 6). Whereas the oxidation process is directly associated with the conjugated structure, i.e. p-doping, the reduction process is irreversible and poorly defined and associated with polymer defects and/or traces of impurities. As such the charge carrier mobility was determined and a promising mobility value of 1.7 10-3 cm2 / Vs was found.

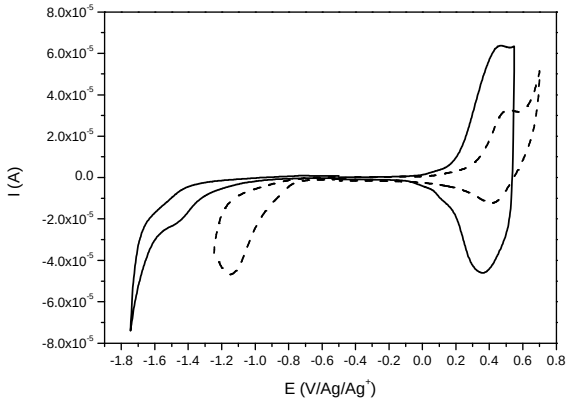

Figure 6 Voltammogram of PTV with R = H (---) and R = Bu (full line)

Solar cells were produced using PCBM as the acceptor material in a 3:1 ratio relative to the PTV polymer. A very interesting Voc was observed of 650 mV with a short circuit current of about 1 mA/cm2. The fill factor was unusually low, only 34%. It may indicate that shunts are dominating the behavior of the device. Improvements of polymerization conditions should in principle allow for improving film forming properties and thus overall performance of the devices. The quite high mobility observed for these materials justified further studies. Concerning the synthesis of PTV derivatives we moved on toward the synthesis of 3-hexyl and 3,4-dihexyl derivatives. But first we focussed on improving the molecular weight characteristics of said PTV type of materials. For that purpose the synthesis was pursued of plain PTV rather then more complex structures.

Entry	# eq LDA	λ max (nm)	M_w (DMF)	PD (DMF)	Temp. (°C)	Yield (%)
1	**1.0**	**527**	**16.874**	**1.8**	**-78**	**45**
2	**1.0**	**392**	**7.386**	**1.3**	**0**	**45**
3	**1.0**	**425**	**8.681**	**1.4**	**rt**	**40**
4[a]	**2.0**	**500**	**209.209**	**4**	**-78**	**50**
			5.342[b]	**1.2**		
5[a]	**3.0**	**525**	**77.437**	**2.5**	**-78**	**60**
			4.595[b]	**1.1**		

[a] bimodal Mw distribution, [b] low molecular weight peak

Table 2: Polymerization results toward poly(Thienylene Vinylene) with LDA as the base.

It was observed that polymerisation of the PTV monomer with LDA as the base leads to rather low molecular weights and in some cases a substantial bimodal behaviour (Table

2). Seemingly in this polymerisation reaction a strong tendency can be observed to follow an anionic mechanism leading to low molecular weight material. However high molecular weights are needed for high quality processing, achieving high mobility and true low band gap behaviour. The use of large excesses of base (2 or 3 equivalent) leads to an improvement but at the same time to introduction of side reactions. Although the yield of polymer found after precipitation in a non-solvent of the precursor material (Figure 3) was something between 40 and 60%, rest fractions showed to be very complex mixtures. This is an indication for the occurrence of side reactions. Also the polymerization had to be performed at -78°C. At higher temperatures a polymer structure was obtained with a large number of structural defects, as could be derived from the absorption maxima that could be found for the conjugated system (<500nm). Work on the synthesis towards 3-hexyl-PTV and 3,4-dihexyl-PTV confirmed these observations to a large extend. Furthermore in these cases a fragmentation process was observed which leads to the loss of the hexyl side chains and thus loss of solubility of the PTV derivatives in conjugated form. In view of the complex synthetic route toward the corresponding monomers (see for example Figure 7.), these findings jeopardize the further use of said chemistry for the synthesis of low band gap materials.

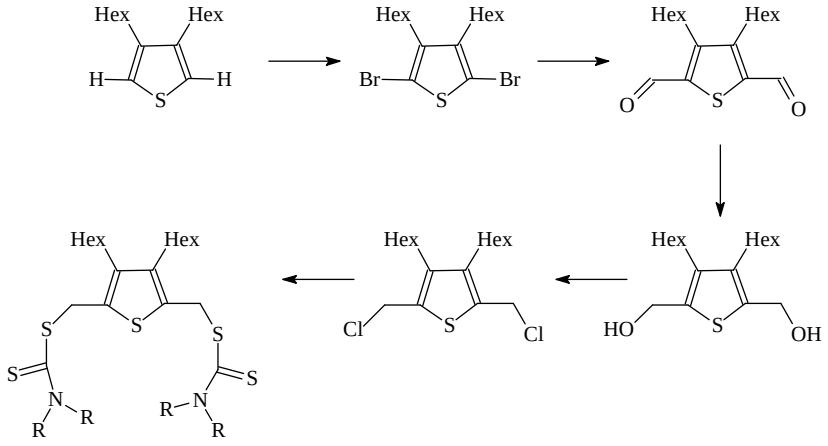

Figure 7: Synthetic route towards the synthesis of the 3,4-dihexylthiophene monomer

In the last year of the project it was discovered that the use of an alternative base, Lithium bis(trimethylsilyl)amide (LiBTMSA), leads to a strong improvement of the characteristics of the dithiocarbamate route. In the synthesis of plain PPV the use of this new base suppresses the anionic mechanism and the occurrence of side reactions. In this way high molecular weight materials are obtained in a reproducible way. Also high quality material can be obtained not only at -78°C but also at 0°C and RT (Table 3). After conversion in film an absorption maximum of 560 nm at RT can be reached, demonstrating high quality development of the conjugated system. The values in Table 3 refer to the absorption maximum at about 200°C, leading to a hypsochromic shift as a consequence of a reversible thermochromic effect. This material also showed in XRD

measurements of the film a clear sign of ordering as indicated by the presence of weak peaks corresponding to distances of 4.4, 3.8 and 3.1 Å.

Entry	Mw	PD	λmax	Condition of polymerization
4	19.799	2.4	476 nm	-78°C 2eq LTSA
5	225.098	8.8	552 nm	0°C 2eq LTSA
6	54.874	5.2	545 nm	R.T. 2 eq LTSA
7	146.903	8.1	523 nm	-78°C 3eq LTSA
8	153.503	6	549 nm	0°C 3eq LTSA
9	43.8724	4.5	530 nm	R.T. 3 eq LTSA

Table 3: Polymerization results toward poly(Thienylene Vinylene) with LTSA as the base.

The corresponding solar cell devices were produced by depositing an active layer in which the PTV precursor together with PCBM in a 1:1 ratio were mixed and subsequently converted to the conjugated polymer. For the best solar cell device a Voc = 350 mV, Isc = 4.85 mA/cm2, a FF = 45% and consequently an efficiency of 0.76% was found.

Extending the use of the new base to the polymerisation of the corresponding 3-hexyl monomer, which is synthesized via a similar route as for the 3,4-dihexyl derivative but then starting from 3-hexylthiophene, confirms earlier observations. Even more importantly no cleavage of the side chains is observed. Data on the polymerisation reactions of the 3-hexyl monomer are displayed in Table 4.

Entry	Mw	PD	λmax	Condition of polymerization
1	50.083	9.6	545 nm	0°C 1.5eq LTSA
2	58.260	7.7	550 nm	0°C 2.0eq LTSA
3	31.950	3.6	566 nm	0°C 1.5eq LTSA
4	35.020	3.7	574 nm	0°C 2.0eq LTSA

Table 4: Polymerization results toward poly(3-HexylThienylene Vinylene) with LTSA as the base.

In all these polymerization a monomer concentration of 0.2 M has been used. When this monomer concentration was doubled a Mw of 97 000 Dalton was found. The data on the absorption maximum are obtained via in situ conversion of the corresponding precursor in a special adapted oven placed in a UV/vis spectrometer. These data represent the absorption maximum at about 200°C. As before due to a thermochromic effect these values are shifted to lower wavelength compared to the value at RT. At room temperature a value of 609 nm is found, indicating the formation of a high quality material on conversion. From the onset of the absorption band an optical band gap of 1.7 eV could be determined. The same values were obtained on conversion of the precursor in o-

dichlorobenzene at reflux for 6 hours (Figure 8). The cyclic voltammogram yields an estimate of the HOMO level at -5.1 eV and the LUMO level at – 3.1 eV. Future work will aim for the evaluation of these materials in solar cells.

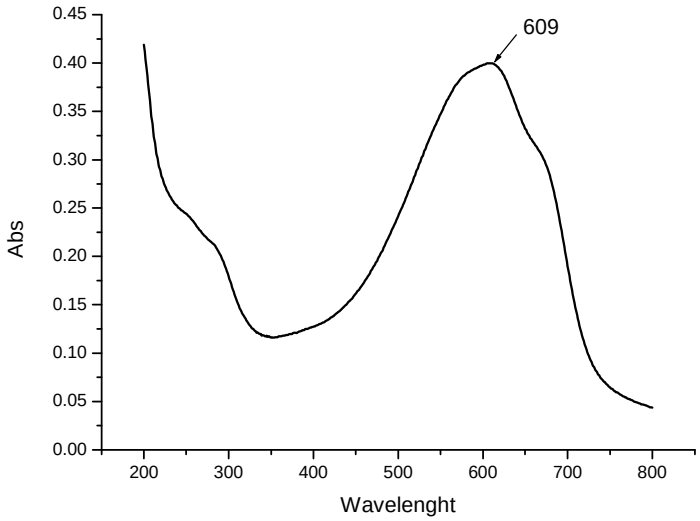

Figure 8: Absorption spectrum at RT in thin film of Poly(2,5-(3-hexyl)Thienylene Vinylene)

As a conclusion of this part it can be stated that within the project “SOLTEX” a breakthrough has been realized concerning the synthesis of Poly(2,5-Thienylene Vinylene) derivatives in general. The use of Lithium Bis(trimethylsilyl)amide as a base, instead of LDA, in the dithiocarbamate precursor route gives rise to the formation of high molecular weight, high quality PTVs (Mw > 40 000 till 100 000, □max > 600nm) with a strong reduction of the occurrence of side reactions. The use of the new base also allows for the synthesis of alkyl substituted PTV derivatives, which are soluble in organic solvents in the conjugated state.

3. Synthesis and characterization of polar p-type conjugated polymers.

It was investigated to what extend more polar type of conjugated polymers can be used in photovoltaic cells. Till now it was established that apolar conjugated polymers, e.g. OC1C10-PPV or P3HT, could in conjunction with fullerene derivatives give rise to fairly efficient solar cells. As mentioned above efficiencies reaching 5% have been demonstrated in literature and by one of the partners (IMEC). However these materials imply processing from highly undesirable solvents like chlorobenzene. To initiate a move to processing procedures which make use of environmentally friendly solvents a shift in the synthesis of active materials was needed. As the class of solvents one would prefer to

use, e.g. alcohols, are mostly more polar, this goal implies the synthesis and study of polar conjugated polymers. For the synthesis of polar PPV derivatives the UHasselt relied on previous work in which a synthetic route was developed for the synthesis of OC1C10-PPV, PEO-PPV, (PEO-OC9)-PPV and (PEO-PEO)-PPVs (Figure 9).

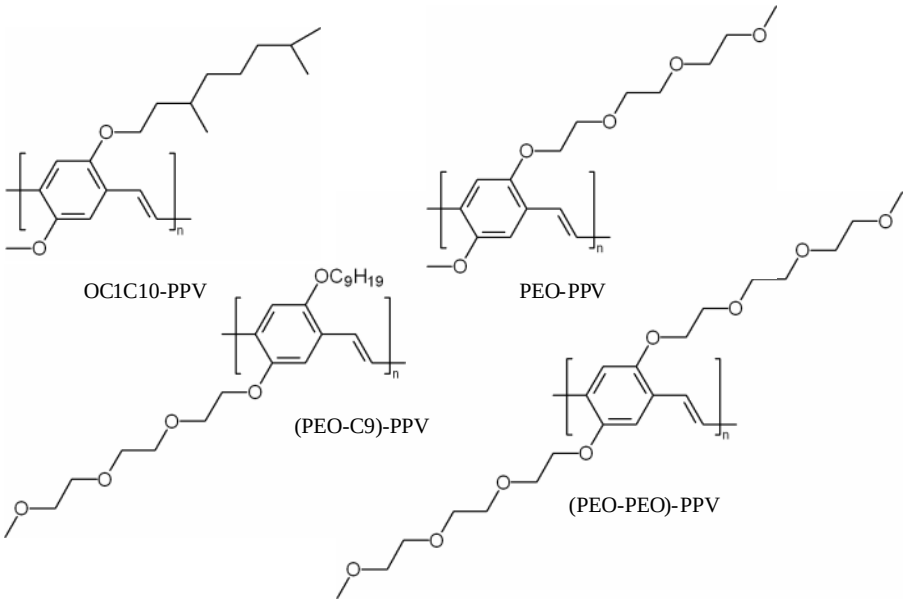

Figure 9: Polar PPV derivatives.

These materials are most conveniently synthesized by the Sulphinyl route (developed at UHasselt) and give rise to materials polymerized in environmental friendly solvents (sec-Butanol) in high yield (50-65%), high molecular weight (300 000 - 450 000 Dalton) with an acceptable polydispersity (PD = 3 - 4). The electrochemical characterization reveals that all these materials have comparable characteristics (Band gap about 2.2 - 2.3 eV, HOMO about -5.2 eV, LUMO about -3.0 eV). From UV/vis spectroscopy a very similar optical band gap was found of about 2.2 eV. On the other hand, except for OC1C10-PPV, all the materials studied show as well reversible oxidation as reduction behavior in electrochemistry. This quite unusual behavior for PPV derivatives is associated most probably with the stabilizing effect for ions of the oligo-ethylene oxide side chains.

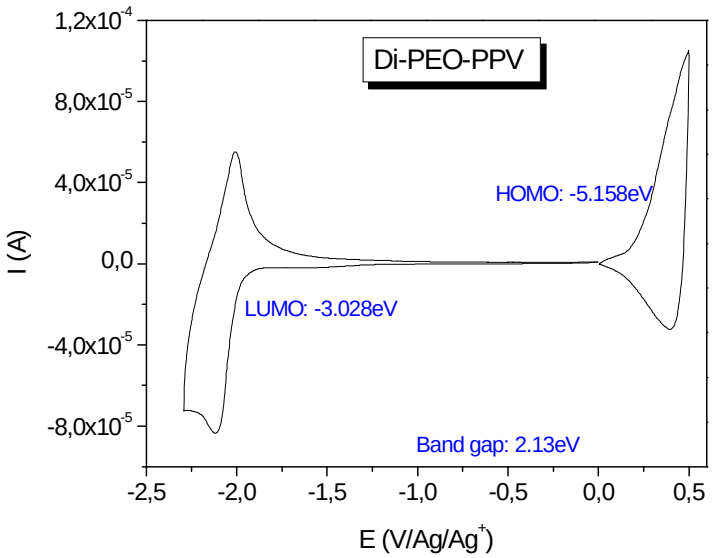

Figure 10: Cyclic voltammogram of di-PEO-PPV

Concerning these polar PPV derivatives, a strong influence was observed of the polarity of the PPV derivative on the morphology of the blend obtained by mixing in PCBM. Using AFM, compared with OC1C10-PPV, a more rough morphology was found (example Figure 11). Seemingly a too drastic change of the relative polarity compared with PCBM must be avoided.

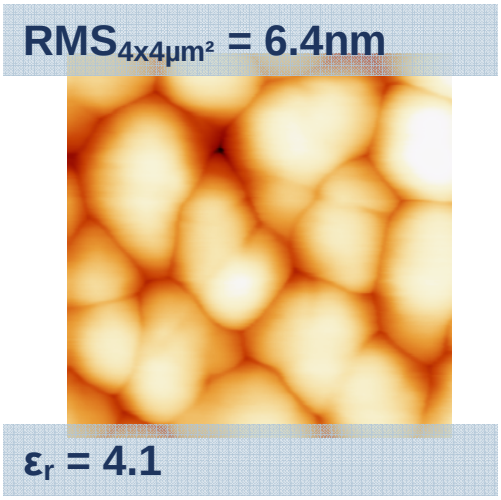

Figure 11 AFM of the morphology of (PEO-OC9)-PPV with PCBM (1:4)

Relative permittivity was used as a measure of changed polarity and was determined to change from 3 for OC1C10-PPV over 4 with one PEO side chain in the PPV backbone to 5.5 for (PEO-PEO)-PPV. The mobility of the polar PPV derivatives synthesized, was determined in a FET-structure and a mobility was found which is independent of the type

of side chain and thus the polarity of the polymer (μfe = 3 10-4 cm2/Vs). Solar cells were produced with said materials and PCBM (1:4). Working solar cells were obtained but with a performance clearly inferior to the standard material OC1C10-PPV (Table 5). Most probably this relates to the coarse morphology observed with AFM and thus an incompatibility of PCBM with such more polar conjugated systems. Future work must be focused on improving morphology by either the use of compatibilizers (surfactants) or more polar fullerene derivatives. Main point in this context is however, that solar cells can be made irrespectively of the polarity of the polymer.

	OC1C10-PPV	**PEO-PPV**	**(PEO-OC9)-PPV**	**(PEO-PEO)-PPV**
RMS 4μm[nm]	*2.3*	*3.8*	*6.4*	*18.0*
jsc [mA/cm2]	*7.0*	*1.8*	*4.3*	*0.006*
Voc [V]	*0.71*	*0.38*	*0.64*	*0.61*
FF [%]	46	26	34	24

Table 5: Solar cell characteristics polar PPV:PCBM (1:4) mixtures

In conclusion PPV derivatives of OC1C10-PPV were synthesized in which apolar side chains were replaced by one or in some cases two oligo ethylene oxide side chains. It was demonstrated that indeed a strong increase of the polarity of the system was achieved by the use of such structures. This resulted finally to the observation that the use of rather polar conjugated polymers can lead to active solar cell devices. On the other hand still further work has to be invested in methods to optimise the morphology. As the polarity increases the timing and extend of phase separation while putting down the active layer is strongly shifted and leads to a less optimal morphology and thus less outstanding performance of said solar cells.

4. Synthesis and characterization of a non-alternant polyaromatic conjugated polymer: a new entry to n-type conjugated polymers.

The dithiocarbamate route was also used in an effort to synthesize a potential n-type conjugated polymer. Most conjugated polymers show a strong p-type behavior, meaning that they show efficient hole transport but weak electron transport. In polymer solar cells the n-type behavior needed for the acceptor component is covered by PCBM, a fullerene derivative. To control efficiently morphology there is an urgent need for acceptor type conjugated polymers. However from literature it is clear that this class of organic semiconductors is less well developed, and a need for new polymer architectures to introduce this behavior in said polymers can be identified.

In this context four classes of such conjugated polymers with potential n-type behavior can be envisaged.

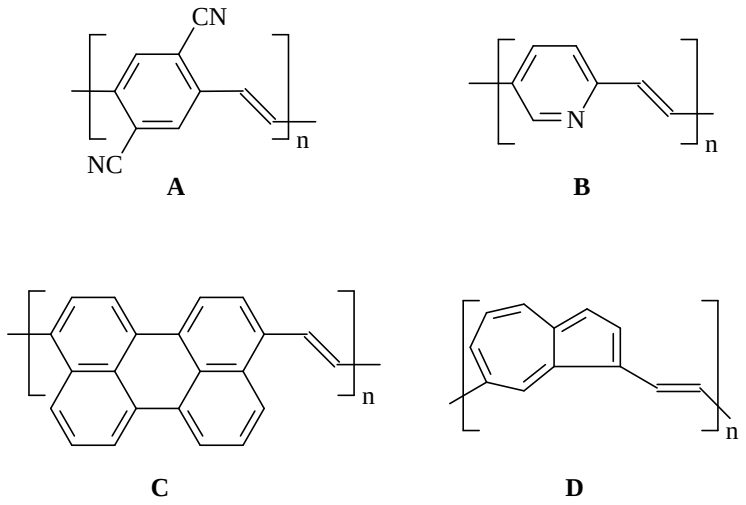

Figure 12: Four general classes of n-type conjugated polymers.

Firstly p-type conjugated polymers like PPV can be converted from a donor to an acceptor type of polymer by substituting strong electron attracting functionalities onto the backbone of the conjugated polymer (Figuur 12, A). Secondly substituting a number of carbon atoms in the conjugated backbone of the conjugated polymer by more electronegative atoms, e.g. nitrogen, can transfer the structure into an acceptor conjugated polymer (Figuur 12, B). Both these approaches are documented in literature to some level. However in principle also polyaromatic structures like Poly(Perylene Vinylene) may form a sound basis for design of n-type conjugated polymers (Figuur 12, C). We opted for a somewhat different approach in the sense that we pursued the synthesis of the backbone of a non-alternant polyaromatic conjugated polymer. In principle a Poly(Azulene Vinylene) type of structure could be an option, but the chemistry of azulene is too complicated to be taken in consideration seriously (Figuur 12, D). We preferred to start work in this domain by designing a synthesis of the non-alternant fluoranthene monomer. The interesting point to stress is that fluoranthene is in fact a substructure of C60. The synthesis route that was developed is depicted in Figuur 13. The first step is a one pot synthesis in which subsequently a Knoevenagel condensation leads in situ to a cyclopentadienone derivative which undergoes a Diels-Alder reaction with the solvent norbornadiene. The final step constitutes a retro-Diels-Alder reaction yielding a fluoranthene derivative that can easily be converted to the corresponding dithiocarbamate monomer via simple chemistry. The synthesis in general proved reproducible and for most steps a good yield could be achieved.

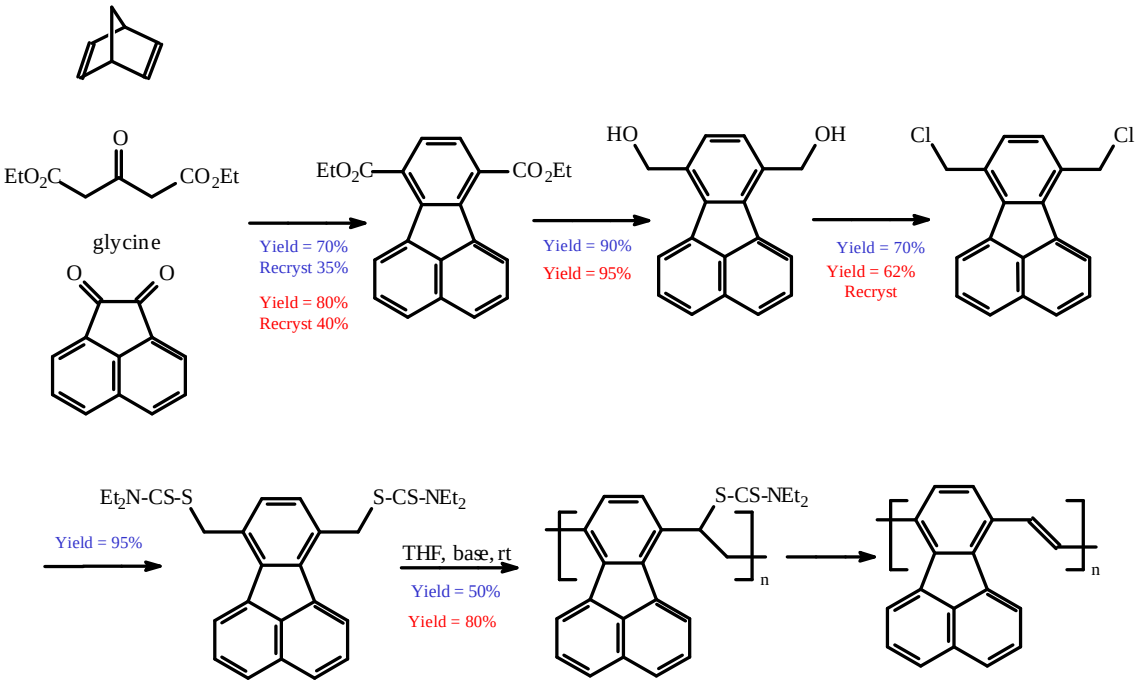

Figure 13: Synthetic route towards the synthesis of the poly(Fluoranthene Vinylene)

Polymerization was performed in THF using the new base, we introduced for the improved synthesis of PTV. A precursor polymer was obtained with a molecular weight of 60 000 Dalton(= Mw) and a polydispersity of 2. No indications were found for a bimodal distribution, demonstrating a clean and straightforward polymerization. The optical band gap was found to be of the order of 2.3 eV and electrochemical characteristics are consistent with the potential of PFV as electron acceptor material (reversible reduction behavior) (Figure 14).

Recently a first attempt was undertaken to synthesize an alkyl-(hexyl) substituted derivative of Poly(Fluoranthene Vinylene). It is expected that an improved solubility of the polymer in conjugated form can be achieved in this way. A precursor polymer could be synthesized with a Mw of 290 000 Dalton and a polydispersity of 2.8. After conversion an optical band gap in film was found of 2.2 eV.

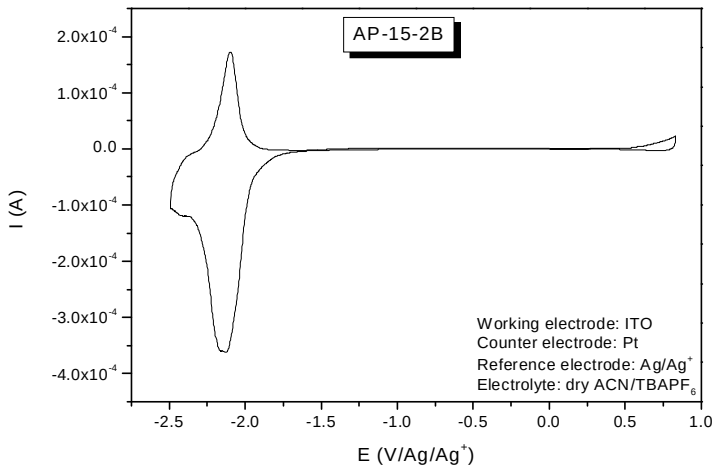

Figure 14: Cyclic Voltammogram of poly(Fluoranthene Vinylene)

In conclusion it could be demonstrated that Poly(Fluoranthene Vinylene) (PFV) can show the characteristics of a potential n-type conjugated polymer. Consequently this class of polymers may be used to develop polymeric acceptor systems for plastic solar cells.

IV. Conclusions

The project goals in the different work packages have been achieved according to schedule. After the preparation and characterization of new materials (discotic liquid crystals and polymers) in the 1st year, advances have been made in the 2nd year concerning screen-printing on flexible substrates, and lamination. The materials characterization and theoretical description has been continued and refined in the 3rd year.

The consortium has published scientific results from the Soltex project and made many presentations at international conferences and workshops.

The process to obtain spincoated phthalocyanine films which display homeotropic alignment is the object of a patent which was deposited by **ULB** on May 15, 2005, with the number 05447108.1 and which is referenced at the ULB as P.ULB.110A/EP.

In collaboration with Samsonite a demonstrator was worked out by **CTB** and **IMEC** to illustrate and promote the project. A suitcase from Samsonite with a textile part was used to integrate a small LCD display powered by solar cells, as shown on the picture below. The suitcase was shown on the Centexbel booth at Techtextile 2005 (Frankfurt, G) and at Flanders Textile Valley 2005 (Kortrijk, B) where Centexbel also organised its "Technologiedag". A similar suitcase will be made for Imec to show in their exhibition room.

V. Dissemination and valorization

A. Partner IMEC

1. First year (2003)

V. Arkhipov, P. Heremans, H. Baessler, "Why is exciton splitting so efficient at the interface between a conjugated polymer and an eectron acceptor?", Applied Physics Letters, Vol. 82, No 25, pp. 4605-4607, 2003

V. Arkhipov, P. Heremans, E. Emelianova, H. Baessler, "Exciton dissociation in doped conjugated polymers", Mat. Es. Symp. Proc. Vol. 771, 2003

Aernouts, T.; Vanlaeke, P.; Poortmans, J. and Heremans, P. Plastic solar cells: screen-printing as a novel deposition technique. Presented at: European Conference on Organic Electronics and Related Phenomena - ECOER. (21-26 September 2003; Wye, Kent, UK.)

Aernouts, T.; Vanlaeke, P.; Geens, W.; Poortmans, J.; Heremans, P.; Borghs, G. and Mertens, R. The influence of the donor/acceptor ratio on the performance of organic bulkheterojunction solar cells. Poster at: E-MRS Spring Meeting Symposium D: Thin Films and Nano-Structured Materials for Photovoltaics. (10-13 June 2003; Strasbourg, France.)

2. Second year (2004)

C. Deibel, S. Put, S. Schols, P. Heremans, V. De Cupere, Y. Geerts, "Charge Transport in the Discotic Liquid Crystal H2Pc(14,10)4". Poster presentation at the Belgian Polymer Group Meeting, May 27-28, 2004 in Houffalize, Belgium.

T. Aernouts, P. Vanlaeke, J. Poortmans, P. Heremans; Polymer solar cells: screen-printing as a novel deposition technique; oral presentation on Symposium about Organic Optoelectronics and Photonics, Photonics-Europe Conference, April 26-30 (2004), Strasbourg, France

T. Aernouts, P. Vanlaeke, J. Poortmans, P. Heremans; Polymer solar cells: screen-printing as a novel deposition technique; oral presentation on MRS Fall meeting, November 29 – December 3 (2004), Boston, MA, USA

V. I. Arkhipov, E. V. Emelianova, and H. Bässler
On the role of spectral diffusion of excitons in sensitized photoconduction in conjugated polymers

Chem. Phys. Lett., 383, 166 (2004).

M. Weiter, V. I. Arkhipov, and H. Bässler
Transient photoconductivity in a thin film of a poly-phenylenevinylene-type conjugated polymer
Synthetic Metals, 141, 165 (2004).

V. I. Arkhipov and H. Bässler
Exciton dissociation and charge photogeneration in pristine and doped conjugated polymers
Phys. Stat. Sol. (a) 201, 1152 (2004).

V. I. Arkhipov, H. Bässler, E. V. Emelianova, D. Hertel, V. Gulbinas, C. Im, and L. Rothberg
Exciton dissociation in conjugated polymers
Macromolecular Symposia, 212, 13 (2004).

V. I. Arkhipov, P .L. Heremans, E. V. Emelianova, and H. Bässler
Spectral diffusion and dissociation of excitons in conjugated polymers
Proceedings of SPIE, 5464, 345 (2004).

V. I. Arkhipov, E. V. Emelianova, and H. Bässler
Quenching of excitons in doped disordered organic semiconductors
Phys. Rev. B, 70, 205205 (2004).

3. Third year (2005)

Screen printing as a deposition technique for flexible polymer solar cell modules; T. Aernouts, P. Vanlaeke, J. Poortmans, P. Heremans; poster presentation on E-MRS conference, May 31- June 3 (2005), Strasbourg, France

Screen printing as a deposition technique for flexible polymer solar cell modules; T. Aernouts, P. Vanlaeke, J. Poortmans, P. Heremans; poster presentation on European Photovoltaics conference, June 6-10 (2005), Barcelona, Spain

P3HT/PCBM bulk heterojunction solar cells: relation between morphology and electro-optical characteristics; P. Vanlaeke, A. Swinnen, I. Haeldermans, G. Vanhoyland, T. Aernouts, D. Cheyns, C. Deibel, J. D´Haen, P. Heremans, J. Poortmans and J. V. Manca, accepted for publication in Solar Energy Materials & Solar Cells

Polythiophene based bulk heterojunction solar cells: morphology and its implications; P. Vanlaeke, G. Vanhoyland, T. Aernouts, D. Cheyns, C. Deibel, J. Manca, P. Heremans and J. Poortmans, accepted for publication in Thin Solid Films

B. Partner CENTEXBEL

1. Second year (2004)

On June 7-8, 2004, Tom Meyvis attended the European Coating Conference "Smart Coatings III" in Berlin. The most recent evolutions in coating technology are presented on this conference. Interesting contributions from A. Hauch (Siemens) on plastic solar cells and from S Amberg-Schwab (Fraunhofer institute for Silicate Research) on high performant plastic barriers for organic electronics.

2. Third year (2005)

F. Pirotte*, M. Belly*,J. Léonard*, M. Catrysse** E2T –Electronic embedded in Textiles: recent developments at Centexbel, 5 th World Textile Conference AUTEX 2005, 27-29 June 2005, Portorož, Slovenia;

Power sources for smarth clothes an overview, M. Catrysse[1], C. Hertleer, K. Van de Voorde, T. Meyvis, T. Aernouts, Ambience 2005, 19-20 september, Tampere Finland.

C. Partner UNIVERSITE LIBRE DE BRUXELLES

1. Third year (2005)

Micro and nanoscale morphology of discotic liquid crystal/fullerene derivatives blends, Vinciane M. De Cupere, Pascal Viville, Alain M. Jonas, Roberto Lazzaroni, Yves H. Geerts. In preparation.

Effect of interfaces on the alignment of a discotic liquid-crystalline phthalocyanine, Vinciane De Cupere, Julien Tant, Pascal Viville, Roberto Lazzaroni, Wojciech Osikowicz, William R. Salaneck, Yves Henri Geerts. In preparation.

Homeotropic Alignment of a Discotic Liquid Crystal Induced by a Sacrificial Layer. Eric Pouzet, Vinciane De Cupere, Christophe Heintz, Martin M. Nielsen, Pascal Viville, Roberto Lazzaroni, William Salaneck, Wojciech Osikowicz, Yves Henri Geerts. In preparation.

D. Partner UNIVERSITE MONS-HAINAUT

1. First year (2003)

J. Cornil, V. Lemaur, M.C. Steel, H. Dupin, A. Burquel, D. Beljonne, and J.L. Brédas. "Electronic Structure of Organic Photovoltaic Materials: Modelling of Exciton Dissociation and Charge Recombination Processes".
In « Organic Photovoltaics : Mechanisms, Materials, and Devices » edited by S. Sun and N.S. Sariciftci (Marcel Dekker, New York), in press

2. Second year (2004)

Electronic Structure of Organic Photovoltaic Materials: Modelling of Exciton Dissociation and Charge Recombination Processes". J. Cornil, V. Lemaur, M.C. Steel, H. Dupin, A. Burquel, D. Beljonne, and J.L. Brédas. In « Organic Photovoltaics: Mechanisms, Materials, and Devices » edited by S. Sun and N.S. Sariciftci (Marcel Dekker, New York), in press.

Charge-Transfer and Energy-Transfer Processes in π-Conjugated Oligomers and Polymers: A Molecular Description". J.L. Brédas, D. Beljonne, S. Coropceanu, and J. Cornil. Chemical Reviews 104 (2004) 4971-5003.

Photoinduced Charge Generation and Recombination Dynamics in Model Donor/Acceptor Pairs for Organic Solar Cell Application: A Full Quantum-Chemical Treatment. V. Lemaur, M.C. Steel, D. Beljonne, J.L. Brédas, and J. Cornil. Journal of the American Chemical Society, in press.

3. Third year (2005)

"Charge-Transfer and Energy-Transfer Processes in π-Conjugated Oligomers and Polymers: A Molecular Description".
J.L. Brédas, D. Beljonne, S. Coropceanu, and J. Cornil.
Chemical Reviews 104 (2004) 4971-5003.

"Electronic Structure of Organic Photovoltaic Materials: Modelling of Exciton Dissociation and Charge Recombination Processes".
J. Cornil, V. Lemaur, M.C. Steel, H. Dupin, A. Burquel, D. Beljonne, and J.L. Brédas.
In « Organic Photovoltaics : Mechanisms, Materials, and Devices » edited by S. Sun and N.S. Sariciftci (Marcel Dekker, New York, 2005), chap. 7, p.161-182.

"Photoinduced Charge Generation and Recombination Dynamics in Model Donor/Acceptor Pairs for Solar Cell Applications: A Full Quantum-Chemical Treatment".
V. Lemaur, M.C. Steel, D. Beljonne, J.L. Brédas, and J. Cornil.
Journal of the American Chemical Society 127 (2005) 6077-6086.

"Liquid Crystalline Metal-Free Phthalocyanines Designed for Charge and Exciton Transport".
J. Tant, Y.H. Geerts, M. Lehmann, V. De Cupere, G. Zucchi, B.W. Laursen, T. Björnholm, V. Lemaur, V. Marcq, A. Burquel, E. Hennebicq, F. Gardebien, P. Viville, D. Beljonne, R. Lazzaroni, and J. Cornil.
Journal of the Physical Chemistry B 109 (2005) 20315-20323.

"Pathways for Photoinduced Charge Generation and Recombination at Donor-Acceptor Heterojunctions: The Case of Oligophenylenevinylene-Perylene Bisimide Complexes".
A. Burquel, V. Lemaur, D. Beljonne, R. Lazzaroni, and J. Cornil.
Journal of Physical Chemistry B, submitted for publication

"Optical Bandgaps of π-Conjugated Organic Materials at the Polymer Limit: Experiment and Theory".
J. Gierschner, J. Cornil, and H.J. Egelhaaf.
In preparation.

E. Partner UNIVERSITEIT HASSELT

1. First year (2003)

D. Vanderzande, M. Knipper, M. Nicolas, A. Henckens, I. Polec, K. Colladet, L. Lutsen, J. Manca, 'Prerequisites and Properties of Low Band Gap Materials towards Photovoltaic Applications', Invited talk E-MRS Spring Meeting 2003, June 10-13 Strassbourg, France.

D. Vanderzande, M. Knipper, M. Nicolas, A. Henckens, I. Polec, K. Colladet, L. Lutsen, J. Manca, 'Low Band Gap Materials for Photovoltaic Applications', Invited talk, Polymers for Advanced Technologies PAT 2003, September 21-24 Ft. Lauderdale, Florida, USA.

"Poly(Thienylene Vinylene) derivatives as low band gap polymers for photovoltaic applications"; A. Henckens, M. Knipper, J. Manca, L. Lutsen, D. Vanderzande, Poster 7th International Symposium on Polymers for Advanced Technology September 21-24, 2003, Radisson Bahia Mar Resort, Fort Lauderdale, Florida, USA

2. Second year (2004)

Conferences attended by LUC team and talks.

"The Polymerisation behaviour of p-Quinodimethane Systems: Competing and conflicting radical and anionic mechanisms"; D. Vanderzande, L. Hontis, L. Lutsen, V. Vrindts, I. Duyssens and T. Cleij, Oral presentation, FPi6- 6th International Symposium on Functional Pi-Elektron Systems; June 14-18, 2004, Ithaca, USA. (Goal: Developing contacts with research groups in the world active in organic semi-conductors, specifically the community involved in Organic Solar Cells)

"The polymerisation behaviour of p-quinodimethyane systems: competing and conflicting radical and anionic mechanisms." D. Vanderzande, Invited Talk at the Symposium on Functional Polymer Materials, organisation BPG-KNCV, 7-8 oktober 2004, Mol, België. (Goal: Developing contacts with research groups in the world active in organic semi-conductors, specifically the community involved in Organic Solar Cells)

"Development of a new synthesis method to poly(thienylene vinylene)"; L.Lutsen, A. Henckens, K.Colladet, D. Vanderzande. Talk at SPIE 2004, Strasbourg, France, 26-30 April 2004. (Goal: Developing contacts with research groups in the world active in organic semi-conductors, specifically the community involved in Organic Solar Cells)

Poster presentations on Conferences attended by LUC team.

"A new synthetic method towards Poly(Thienylene Vinylene) derivatives and their application in organic photovoltaics"; D. Vanderzande, A. Henckens, L. Lutsen, Poster presentation, FPi6- 6th International Symposium on Functional Pi-Elektron Systems; June 14-18, 2004, Ithaca, USA.

"Mesoscopic order in pi-conjugated PPV-derivatives"; L. Breban, L. Lutsen, D. Vanderzande, Poster presentation, Symposium on functional polymer materials, 7-8 oktober 2004, Mol, België

"Soluble low-band gap polymers for solar cell applications via oxidative polymerisations"; K. Collatdet, L. Lutsen, D. Vanderzande, Poster presentation, Symposium on functional polymer materials, 7-8 oktober 2004, Mol, België

"Synthesis of low band gap materials based on thiophene derivatives"; F. Banishoeib, L. Lutsen, D. Vanderzande, Poster presentation, Symposium on functional polymer materials, 7-8 oktober 2004, Mol, België

"Synthesis of poly(thienylene vinylene) (PTV) via the dithiocarbamate route, a new precursor route towards conjugated polymers"; A. Henckens, M. Knipper, J. Manca, T. Aernouts, J. Poortmans, L. Lutsen, D. Vanderzande, , Poster presentation Symposium on functional polymer materials, 7-8 oktober 2004, Mol, België

"Poly(thienylene vinylene) derivatives as low band gap polymers for photovoltaic applications"; A. Henckens, M. Knipper, J. Manca, L. Lutsen, D. Vanderzande, Poster presentation, Symposium on functional polymer materials, 7-8 oktober 2004, Mol, België

"Synthesis of n-type conjugated polymers; Poly(quinoxaine vinylene)"; Z. Olomi, L. Lutsen, D. Vanderzande, Poster presentation, Symposium on functional polymer materials, 7-8 oktober 2004, Mol, België

Publications by LUC team in 2004

Henckens, A; Adriaensens, P; Gelan, J; Lutsen, L; Vanderzande, D; "Synthesis and complete NMR spectral assignment of thiophene-substituted sulfinyl monomers", MAGNETIC RESONANCE IN CHEMISTRY; (2004) 42 (11), 931-937

Adriaensens, P; Dams, R; Lutsen, L; Vanderzande, D; Gelan, J; "Study of the nanomorphology of OC1C10-PPV/precursor-PPV blends by solid state NMR relaxometry"; POLYMER; (2004) 45 (13), 4499-4505

Aubert, PH; Knipper, M; Groenendaal, L; Lutsen, L; Manca, J; Vanderzande, D; "Copolymers of 3,4-ethylenedioxythiophene and of pyridine alternated with fluorene or phenylene units: Synthesis, optical properties, and devices"; MACROMOLECULES; (2004) 37 (11), 4087-4098

Colladet, K; Nicolas, M; Goris, L; Lutsen, L; Vanderzande, D; "Low-band gap polymers for photovoltaic applications"; THIN SOLID FILMS; (2004) 451-52; 7-11

Geens, W; Martens, T; Poortmans, J; Aernouts, T; Manca, J; Lutsen, L; Heremans, P; Borghs, S; Mertens, R; Vanderzande, D; "Modelling the short-circuit current of polymer bulk heterojunction solar cells"; THIN SOLID FILMS; (2004) 451-52; 498-502

Henckens, A; Knipper, M; Polec, I; Manca, J; Lutsen, L; Vanderzande, D; "Poly(thienylene vinylene) derivatives as low band gap polymers for photovoltaic applications", THIN SOLID FILMS; (2004) 451-52, 572-579

Martens, T; Munters, T; Goris, L; D'Haen, J; Schouteden, K; D'Olieslaeger, M; Lutsen, L; Vanderzande, D; Geens, W; Poortmans, J; De Schepper, L; Manca, JV; Nanostructured organic pn junctions towards 3D photovoltaics"; APPLIED PHYSICS A-MATERIALS SCIENCE & PROCESSING; (2004) 79 (1) 27-30

Riedel, I; Parisi, J; Dyakonov, V; Lutsen, L; Vanderzande, D; Hummelen, JC; "Effect of temperature and illumination on the electrical characteristics of polymer-fullerene bulk-heterojunction solar cells"; ADVANCED FUNCTIONAL MATERIALS; (2004) 14 (1) 38-44

Pientka, M; Dyakonov, V; Meissner, D; Rogach, A; Vanderzande, D; Weller, H; Lutsen, L; Vanderzande, D; "Photoinduced charge transfer in composites of conjugated polymers and semiconductor nanocrystals"; NANOTECHNOLOGY; (2004) 15 (1) 163-170

Mozer, A; Denk, P; Scharber, M; Neugebauer, H; Sariciftci, S; Wagner, P; Lutsen, L; Vanderzande D; "Novel regiospecific MDMO-PPV copolymer with improved charge transport for bulk heterojunction solar cells"; J. PHYS. CHEM. B; (2004), 108; 5235-5242

Henckens, L. Lutsen, D. Vanderzande, M. Knipper, J. Manca, T. Aernouts, J. Poortmans. "Synthesis of PTV via the dithiocarbamate route, a new precursor route towards conjugated polymers." Proc. SPIE Int. Soc. Opt. Eng. 5464 (2004) 52-59

3. Third year (2005)

L. Goris, K. Haenen, M. Nesladek, P. Wagner, D. Vanderzande, L. De Schepper, J. D'Haen, L. Lutsen, J.V. Manca, "Absorption phenomena in organic thin films for solar cell applications investigated by photothermal deflection spectroscopy", Journal of Materials Science 40/6 (2005) 1413-1418

Mozer AJ, Sariciftci NS, Lutsen L, Vanderzande D, Osterbacka R, Westerling M, Juska G , "Charge transport and recombination in bulk heterojunction solar cells studied by the photoinduced charge extraction in linearly increasing voltage technique", APPLIED PHYSICS LETTERS (2005) 86 (11): Art. No. 112104

Adriaensens P, Roex H, Vanderzande D, Gelan J, "Study of the thermal elimination process of sulphinyl-based PPV precursors by solid state NMR", POLYMER (2005) 46 (6): 1759-1765

Mozer, AJ; Denk, P; Scharber, MC; Neugebauer, H; Sariciftci, NS; Wagner, P; Lutsen, L; Vanderzande, D; Kadashchuk, A; Staneva, R; Resel, R; "Novel regiospecific MDMO-PPV polymers with improved charge transport properties for bulk heterojunction solar cells"; SYNTHETIC METALS, (2005) 153 (1-3): 81-84 Part 2 Sp. Iss.

Kesters E, Vanderzande D, Lutsen L, Penxten H, Carleer R , "Study of the thermal elimination and degradation processes of n-alkylsulfinyl-PPV and -OC1C10-PPV precursor polymers with in situ spectroscopic techniques", MACROMOLECULES (2005) 38 (4): 1141-1147

Henckens A, Colladet K, Fourier S, Cleij TJ, Lutsen L, Gelan J, Vanderzande D, "Synthesis of 3,4-diphenyl-substituted poly(thienylene vinylene) low-band-gap polymers via the dithiocarbamate route", MACROMOLECULES (2005) 38 (1): 19-26

Van Severen, I; Motmans, F; Lutsen, L; Cleij, TJ; Vanderzande, D; "Poly(p-phenylene vinylene) derivatives with ester- and carboxy-functionalized substituents: a versatile platform towards polar functionalized conjugated polymers"; POLYMER, (2005) 46 (15): 5466-5475.

Dirk J. M. Vanderzande, Lieve Hontis, Arne Palmaerts, David Van Den Berghe, Jimmy Wouters, Laurence Lutsen and Thomas Cleij, "Block-type architectures for Poly(p-Phenylene Vinylene) derivatives: A reality or an illusion?", SPIE-Organic Light-Emitting Materials and Devices IX, edited by Zakya H. Kafafi, Paul A. Lane, Proc. of SPIE Vol. 5937, 59370Q, (2005)

Seminars organized

Seminar at UHasselt ""Physics of Polymeric Devices: Part I" door prof. Dr. Paul W.M. Blom Materials Science Centre (Physics of Organic Semiconductors), University of Groningen, Nederland op 4 february 2005.

Seminar at UHasselt ""Physics of Polymeric Devices: Part II" door prof. Dr. Paul W.M. Blom Materials Science Centre (Physics of Organic Semiconductors), University of Groningen, Nederland op 4 february 2005.

Lectures delivered

Dirk J. M. Vanderzande, Lieve Hontis, Arne Palmaerts, David Van Den Berghe, Jimmy Wouters, Laurence Lutsen and Thomas Cleij, "Block-type architectures for Poly(p-Phenylene Vinylene) derivatives: A reality or an illusion?", SPIE-Optics & Photonics 2005-Organic Light-Emitting Materials and Devices IX, 31 July-4 August 2005, San Diego, USA

Dirk J. M. Vanderzande, "The dual behaviour in the polymerization reactions of p-quinodimethanesystems", 1st Korea-Belgium Bilateral Symposium on Functional Polymers, 24-25 October, Korea University, Seoul, Korea.

Sofie Fourier, Fateme Banishoeib, Ineke Van Severen, Thomas Cleij, D. Vanderzande, "Opto-electronic characterisation of various PPV- and PTV-derivatives", BPG-2005, 19-20th mei 2005, La-Roche-en-Ardenne, Belgium

A. Swinnen, I. Haeldermans, P. Vanlaecke, J. D'Haen, G. Vanhoyland, M. D'Olieslaeger, J.V. Manca, J. Mullens, J. Poortmans, D. Vanderzande 'Influence of post-production annealing on the morphology of polythiophene/fullerene bulk heterojunction solar cells', ICOE05, Eindhoven, Nederland, 21-24 June 2005.

VI. Patents and products

The process to obtain spincoated phthalocyanine films which display homeotropic alignment is the object of a patent which was deposited by **ULB** on May 15, 2005, with the number 05447108.1 and which is referenced at the ULB as P.ULB.110A/EP.

In collaboration with Samsonite a demonstrator was worked out by **CTB** and **IMEC** to illustrate and promote the project. A suitcase from Samsonite with a textile part was used to integrate a small LCD display powered by solar cells, as shown on the picture below. The suitcase was shown on the Centexbel booth at Techtextile 2005 (Frankfurt, G) and at Flanders Textile Valley 2005 (Kortrijk, B) where Centexbel also organised its "Technologiedag". A similar suitcase will be made for Imec to show in their exhibition room.